



Injectable hypoxia-preconditioned cartilage progenitor cells-laden GelMA microspheres system for enhanced osteoarthritis treatment



Kai Feng^{a,1}, Yifan Yu^{a,1}, Zhengsheng Chen^{a,1}, Feng Wang^a, Kunqi Zhang^a, Hongfang Chen^b, Jia Xu^{a,**}, Qinglin Kang^{a,*}

^a Department of Orthopedic Surgery, Shanghai Sixth People's Hospital Affiliated to Shanghai Jiao Tong University School of Medicine, Shanghai, 200233, China

^b Department of Orthopaedics, Shanghai Tenth People's Hospital, Tongji University, Shanghai, 200072, China

ARTICLE INFO

Keywords:

Osteoarthritis
Cartilage progenitor cells
Hypoxia
Three-dimensional culture
Cartilage tissue engineering

ABSTRACT

Osteoarthritis (OA) is the most common age-related degenerative joint disease mainly characterized by the destruction of articular cartilage. Owing to its native avascular property, intrinsic repair of articular cartilage is very limited. Thus, a chondrogenic microenvironment in the joint is essential to the preservation of healthy chondrocytes and OA treatment. Recently, cartilage progenitor cells (CPCs)-based therapy is emerging as a promising strategy to repair degenerated and damaged articular cartilage. In this study, injectable hypoxia-preconditioned three-dimensional (3D) cultured CPCs-laden gelatin methacryloyl (GelMA) microspheres (CGMs) were constructed and characterized. Compared to normoxia-pretreated 3D CPCs and two-dimensional (2D) cultured CPCs, hypoxia-preconditioned 3D cultured CPCs exhibited enhanced cartilage extracellular matrix (ECM) secretion and greater chondrogenic ability. In addition, hypoxia-preconditioned 3D cultured CPCs more effectively maintained cartilage matrix metabolism balance and attenuated articular cartilage degeneration in subacute and chronic rat OA models. Mechanistically, our results demonstrated hypoxia-preconditioned 3D cultured CPCs exerted chondro-protective effects by inhibiting inflammation and oxidative stress via NRF2/HO-1 pathway *in vitro* and *in vivo*. Together, through the 3D culture of CPCs using GelMA microspheres (GMs) under hypoxia environment, our results proposed an efficient articular cartilage regeneration strategy for OA treatment and could provide inspiration for other stem cells-based therapies.

1. Introduction

Osteoarthritis (OA) is the most common joint disease in aged people and primarily characterized by progressive degeneration and loss of articular cartilage [1]. The OA pathogenesis is generally related to aging and abnormal mechanical stress-induced oxidative stress in cartilage [2, 3]. Numerous studies have demonstrated that both aging and abnormal mechanical stress promote accumulation of reactive oxygen species (ROS) and cause excessive oxidative stress in cartilage, which in turn result in cartilage extracellular matrix (ECM) metabolism imbalance and chondrocyte apoptosis, ultimately leading to cartilage destruction and OA progression [4]. To date, there is no disease-modifying drug available for OA patients in clinic [5]. Thus, it is urgent and crucial to explore efficacious treatments to prevent and alleviate OA development.

Cell-based tissue engineering therapy is a promising strategy to

promote cartilage repair and regeneration [6–8]. Recently, there is a growing body of evidence that cartilage progenitor cells (CPCs) are a novel cell population isolated from articular cartilage, exhibiting self-proliferative capacity and chondrogenic differentiation ability [9, 10]. CPCs play an essential role in the development, maturation, and repair of articular cartilage. Moreover, CPCs present a low expression of the transcription factor RUNX2 which is crucial to the terminal differentiation of chondrocyte and formation of calcified bone tissue [11,12]. Therefore, CPCs can resist to hypertrophy and produce hyaline-like cartilage persistently. Additionally, an *in vitro* study showed CPCs effectively decreased the expressions of inflammatory factors (IL6, MCP-1, and IL-1 β) and matrix metalloproteinases (MMPs), while it significantly up-regulated the expression of cartilage ECM marker collagen II in IL-1 β -induced human chondrocytes [13]. These evidences demonstrate CPCs are promising seeding cells for cartilage tissue engineering in OA

* Corresponding author.

** Corresponding author.

E-mail addresses: xujia0117@126.com (J. Xu), orthokang@163.com (Q. Kang).

¹ The first three authors (Kai Feng, Yifan Yu, and Zhengsheng Chen) contributed equally to this work.

treatment. Although CPCs showed many unique advantages in cartilage regeneration, current studies on the potential of CPCs for tissue engineering is still limited. In a previous study, gelatin methacryloyl (GelMA)-based hydrogels were applied to culture CPCs *in vitro*, and CPCs showed low expression of a hypertrophy marker collagen X and a high expression of lubricin (also named PrG4) and cartilage ECM glycosaminoglycan (GAG) contents [14]. A recent study demonstrated that combining CPCs with poly(3-hydroxybutyrate-co-3-hydroxyvalerate) (PHBV) effectively promoted chondrocyte proliferation and the formation of typical cartilage structure [15]. Taken together, previous studies provide important evidences for the possible clinic application of CPCs in regenerative medicine, and pave the way to CPCs-based cartilage tissue engineering strategy for cartilage repair and OA treatment.

The conventional method for obtaining therapeutic stem cells is mainly based on two-dimensional (2D) culture technology where cells adhere on substrate as a monolayer mode. However, 2D culture condition cannot simulate the actual physiological environment of stem cells niche and it severely hampers the therapeutic potentials of stem cells in tissue repair and regeneration [16–18]. Therefore, it is essential to maintain the stemness and maximize the efficacy of cultured stem cells before harvesting these cells. Three-dimensional (3D) culture technology can mimic a more actual and beneficial physiological environment through cell to cell and cell to matrix interaction [19–21]. In addition, previous studies have demonstrated that mesenchymal stem cells (MSCs) cultured in 3D condition possess an enhanced stemness and improved therapeutic effects [14,22]. Previous study showed that 3D cultured bone marrow-derived MSCs in the poly(lactic acid-co-glycolic acid) (PLGA)-templated collagen scaffolds significantly promoted the expressions of chondrogenesis-related genes and the production of cartilage matrix [22]. Additionally, 3D cultured equine bone marrow-derived MSCs as spheroids possess higher amounts of anti-inflammatory and anti-apoptotic factors than 2D cultured MSCs, and thus enhance their anti-inflammatory property [23]. Therefore, 3D cultured CPCs may hold the advantages of greater chondrogenic ability and chondro-protective effects, which will show stronger therapeutic potentials in OA treatment.

Oxygen concentration is known to be an important external factor which can regulate the proliferation, differentiation, and self-renewal of mesenchymal stem cells (MSCs) and other stem cells [24]. It has been reported that hypoxia pretreatment of MSCs is a beneficial strategy to promote cell survival, proliferation, growth factors secretion, and tissue regeneration [25–27]. Recent studies have showed that hypoxic preconditioning enhanced the function of MSCs, which significantly promoted cartilage repair and alleviate OA progression [28,29]. *In vitro* cultured CPCs in previous research are exposed to normal oxygen concentration (21%, normoxia) conventionally, while the concentration of oxygen in the joint cavity is 1% (hypoxia), which means CPCs reside in a hypoxic micro-environment [30]. Therefore, it was hypothesized that hypoxia-pretreatment might improve the biological function of CPCs.

Nuclear factor (erythroid-derived 2)-like 2 (NRF2) is an essential regulator that maintains cellular homeostasis by regulating oxidative stress and inflammatory responses [31–34]. Under physiological condition, NRF2 combines with the Kelch-like ECH-associated protein1 (KEAP1) which restricts the localization of NRF2 to cytoplasm. Under cellular stress, NRF2 is liberated from KEAP1 and translocate into the nucleus, and then bind to the antioxidant response element to promote the expressions of different antioxidant markers, including heme oxygenase-1 (HO-1) and NADPH quinone oxidoreductase 1 (NQO1). Previous studies indicated that NRF2 activation provided beneficial effects in degenerative diseases, such as neurodegenerative diseases and intervertebral disc degeneration [35,36]. Recently, numerous research has demonstrated that NRF2 is a protective factor that exerts anti-oxidative and anti-inflammatory effects in OA cartilage and activation of NRF2 relieves inflammatory responses and oxidative stress in chondrocytes [37–39]. Thus, it is important to explore whether 3D cultured CPCs under hypoxic condition could exert protective effects on chondrocytes by NRF2/HO-1 signaling pathway.

In this study, we isolated rat CPCs and constructed 3D culture system by using gelatin methacryloyl (GelMA) microspheres (GMs). Next, we compared the chondrogenic ability and chondro-protective effects of hypoxia-pretreated 3D cultured CPCs and normoxia-pretreated 3D cultured CPCs *in vitro*. Our results demonstrated that hypoxia-preconditioned 3D cultured CPCs exhibited enhanced cartilage ECM secretion and greater chondrogenic ability, compared to 2D cultured CPCs and normoxia-pretreated 3D cultured CPCs. Additionally, intra-articular injection of 3D cultured CPCs-laden gelatin methacryloyl (GelMA) microspheres (CGMs) more effectively maintained ECM metabolism balance and ameliorated cartilage destruction in both subacute and chronic rat OA models. Moreover, hypoxia-preconditioned 3D cultured CGMs exerted strong chondro-protective effects by inhibiting inflammation and oxidative stress via NRF2/HO-1 pathway *in vitro* and *in vivo*. Collectively, through the 3D culture of CPCs using GMs under hypoxic environment, our work may provide new insights in CPCs-based therapy for OA treatment.

2. Materials and methods

2.1. Materials

Dulbecco's modified Eagle's medium (DMEM)-F12 and phosphate buffered saline (PBS) were supplied by HyClone (USA). Fetal bovine serum (FBS), collagenase II, and Penicillin-Streptomycin (P.S.) were purchased from Gibco (USA). Transforming growth factor-beta 2 (TGF- β 2) and fibroblast growth factor-2 (FGF-2) were obtained from Biovision (USA). Interleukin-1 β (IL-1 β) was obtained from R&D system (USA). 0.25% trypsin was obtained from Invitrogen (USA). Bovine Serum Albumin (BSA), fibronectin, ascorbic acid, L-glutamine, NRF2 inhibitor Brusatol, and dimethyl sulfoxide (DMSO) were purchased from Sigma (USA). 4% paraformaldehyde (PFA) was obtained from servicebio (China). 4',6-diamidino-2-phenylindole (DAPI) and phalloidine were purchased from Beyotime Biotechnology (China). Cell Counting Kit-8 (CCK8) was obtained from Dojindo (Japan). Lipid Peroxidation Malondialdehyde (MDA) Assay Kit and Reactive Oxygen Species (ROS) Assay Kit were purchased from Beyotime (China). Gelatin Methacryloyl (GelMA) Crosslinked Microsphere (EFL-MS-C-GM-50) was obtained from the Suzhou Intelligent Manufacturing Research Institute (China).

2.2. Scanning electron microscopy (SEM)

Scanning electron microscope (SEM) was used to observe the surface morphology and structure of the GelMA Crosslinked Microspheres (GMs). First, the microspheres were coated with gold by using the HitachiMC1000 Ion Sputter Coater for 2 min. Then the GelMA microspheres were scanned by a scanning electron microscope (SEM; GEMINI 300) at an acceleration voltage of 5 kV. Each sample was repeated 3 times.

2.3. Isolation, culture, and identification of CPCs

Ethical approval for this work was obtained from the Independent Ethics Committee of Shanghai Jiao Tong University Affiliated Sixth People's Hospital (Approval Number: 2020-YS-154, March 30, 2020, China). Rat CPCs were isolated from the superficial layer of 8-week-old Sprague-Dawley (SD) rat articular cartilage by the fibronectin adhesion method as previously reported. Briefly, articular cartilage from rat femoral head was subjected to serial enzymatic digestion with 0.25% trypsin and 0.25% collagenase II. The single cells were subjected to differential adhesion on 10 μ g/ml fibronectin pre-coated plates for 30 min. Subsequently, the media and non-adherent cells were discarded and replaced with standard CPCs growth media (DMEM-F12 containing 100 IU/ml P.S., 10% FBS, 2.5 mM/L-glutamine, 62 μ g/ml ascorbic acid, and 2 μ g/ml amphotericin-B). The adherent cells were maintained for 12 days to obtain CPC colonies (>32 cells). CPCs were cultured in normal oxygen

cell incubators (37 °C; 5% CO₂) with 21% O₂ (normoxic condition) or in hypoxic cell incubators (37 °C; 5% CO₂) with 1% O₂ (hypoxic condition). To identify rat CPCs, immunofluorescence staining for CD105 and PRX1 were performed in CPCs. In addition, flow cytometry for CD29, CD44, CD105, CD90, CD45, CD146 were detected and analyzed.

2.4. CPCs culture on the GMs

First, 3 mg of GelMA microspheres were added to each well of a low-adhesion 24-well plate (EFL-TCP-0024, China), and the plate was sterilized by ultraviolet light in a biological safety cabinet for 60 min. Next, 400 µl of DMEM-F12 culture medium was added to each well of the culture plate for 30 min. The microspheres in a 37 °C incubator for 30 min for swelling. Then, 100 µl 2.5 × 10⁵ CPCs suspension was added to each well and mixed with the microspheres under normoxic or hypoxic culture condition.

2.5. Biocompatibility and cytotoxicity assay

To evaluate the biocompatibility and cytotoxicity of the GelMA microspheres, CPCs were seeded on the GMs in a low-adhesion 24-well plate (EFL-TCP-0024, China). The cytotoxicity of the GMs was detected through the viability of CPCs using CCK8 assay after incubating for 3 d, 6 d, and 9 d.

2.6. Cell viability of CPCs

After culture in GMs under normoxic or hypoxic condition for 28 days, the cell viability of CPCs was detected and analyzed. Briefly, the dye solution was prepared by adding 2 µl calcein-AM (YEASEN) and 2 µl propidium iodide (PI; YEASEN) into 4 ml PBS. Next, CPCs were stained with 200 µl dye solution and incubated at 37 °C in the dark for 30 min. Images were observed and captured by the confocal scanning microscopy (Leica microsystems), live and dead CPCs were quantified by using the ImageJ software and the cell viability was calculated and analyzed.

2.7. Chondrogenic ability of CPCs

Chondrogenic induction of CPCs under different conditions were performed as previously reported [40,41]. In brief, CPCs were harvested and incubated in the chondrogenic induction medium (1% vol/vol insulin-transferrin-sodium selenite, 10⁻⁷ M dexamethasone, 1 mM sodium pyruvate, 50 µM ascorbate-2-phosphate, 50 µg/ml proline, and 20 ng/ml transforming growth factor (TGF)-β3) for 28 days. After chondro-induction, anabolism-related biomarkers (*Col2a1* and *Acan*) and chondrogenic genes (*Gdf5*, *Prg4*, *Sox6*, and *Sox9*) were detected to evaluate the chondrogenic ability.

2.8. Chondrocyte isolation and culture

Chondrocytes were harvested from the femoral head of 8-week-old SD rats. Briefly, the harvested articular cartilage was washed with PBS and cut into 1 mm³ by using sterile scalpel, followed by incubation with 0.25% trypsin for 30 min and digestion with 0.25% collagenase II for 4 h at 37 °C. Next, the dissociated chondrocytes were resuspended and filtered through a 40 µm cell filter before seeding at a density of 2 × 10⁵ cells/ml. To induce inflammatory response and oxidative stress *in vitro*, 10 ng/ml IL-1β was applied to rat chondrocytes for 24 h as previously reported [42,43].

2.9. Co-culture of chondrocytes and CPCs

For indirect co-culture of chondrocytes and CPCs, IL-1β-induced chondrocytes were seeded into the lower chamber of transwell and CPCs under different culture conditions were seeded into the upper chamber of transwell (Corning, 0.4 µm). IL-1β-induced chondrocytes were used as

the control group. After co-culture for 48 h, extracellular matrix metabolism-related genes (*Col2a1*, *Acan*, *Prg4*, *Mmp3*, *Mmp13*, and *Adamts5*) were detected and analyzed in all groups.

2.10. Chondrocyte proliferation assay

For cell proliferation assay, IL-1β-activated chondrocytes were seeded into bottom well of a 24-well transwell system at density of 4000 cells/well, and CPCs under different conditions were seeded on the transwell insert with 0.4 µm pore at density of 2000 cells/cm². Cells were cultured for 48 h. Next, 40 µl of CCK8 solution was added into the medium and incubated at 37 °C for 4 h in the dark. The absorbance was detected at 450 nm by a multi-functional microplate reader (Thermo Fisher Scientific, USA). Cell viability was calculated using the following equation:

$$\text{Cell viability (\%)} = (\text{Absorbance sample} / \text{Absorbance control}) \times 100$$

2.11. PCR analysis

Total RNA in rat chondrocytes was extracted by using Trizol (Invitrogen). Reverse transcription and real-time PCR reaction were performed as described previously [44,45]. By correcting the Ct (threshold cycles) values of the target genes to the Ct value of *Gapdh*, ΔCt value was calculated in each group and relative mRNA expressions of all target genes were detected and expressed as 2^{ΔΔCt} with respect to the control group. The primers used in our study were designed and synthesized by Sangon (China) and listed in Table S1.

2.12. Western blot analysis

After different treatments, rat chondrocytes were washed thrice with PBS, and RIPA solution (Beyotime, China) was added in each group to extract total protein and the protein concentration was detected by the classical BCA method [43,44]. 20 µg protein samples were loaded on sodium dodecyl sulfate-polyacrylamide gel electrophoresis (SDS-PAGE) gel and transferred to 0.22 µm polyvinylidene fluoride membrane (PVDF) membranes. Next, the membranes were blocked with 5% BSA solution for 30 min and then incubated with various primary antibodies overnight at 4 °C. The primary antibodies Collagen2 (Abcam, USA), Aggrecan (Abcam, USA), GDF5 (Abcam, USA), PRG4 (Abcam, USA), SOX9 (Proteintech, USA), ADAMTS5 (Abcam, USA), MMP13 (Abcam, USA), TNFα (Abcam, USA), IL6 (Abcam, USA), SOD1 (Proteintech, USA), KEAP1 (Abcam, USA), NRF2 (Abcam, USA), HO-1 (Abcam, USA), β-actin (Abcam, USA), and horseradish peroxidase (HRP)-conjugated secondary antibody were used. Finally, a chemiluminescence reagent (Beyotime, China) was applied to observe and analyze the bands.

2.13. Measurement of sulfated glycosaminoglycan (GAG) and collagen content

The content of GAG and collagen in all groups were detected and analyzed according to previously reported methods [15,41]. First, the DNA content was detected against standard curves of calf thymus DNA (Sigma, USA). Then the total content of sulfated GAG was detected by the dimethylmethylene blue assay and the GAG content was calculated in each group based on the standard curve obtained from chondroitin 6-sulfate from shark (Sigma, USA). Besides, the collagen content in each group was quantified by detecting the content of hydroxyprolin (HYP) and the HYP content was examined against a standard curve of L-HYP (Sigma, USA). The GAG and HYP content were both normalized by the ds-DNA content.

2.14. Immunofluorescence staining

Cells were fixed with 4% PFA for 30 min at room temperature, permeabilized with 0.25% Triton-X 100 for 15 min. Next, the cells were

blocked with 5% BSA for 1 h and incubated at 4 °C overnight with primary antibodies against CD105 (1:200; Abcam), PRX1 (1:200; Abcam), NRF2 (1:100; Abcam). Subsequently, the cells were incubated with secondary antibodies labeled with Alexa 488 or Alexa 546 for 1 h followed by 10 min incubation with DAPI for nuclear staining in the dark at room temperature. Fluorescence images in each group were observed and captured by a confocal microscopy (Leica microsystems).

2.15. Measurement of intracellular ROS

The level of ROS was quantified by the ROS Assay Kit as described previously [45]. 2',7'-Dichlorodihydrofluorescein diacetate (DCFH-DA) is oxidized by ROS in viable rat chondrocytes to 2',7'-dichlorofluorescein (DCF) which is highly fluorescent at 530 nm. First, rat chondrocytes were washed with PBS. Next, 10 μM DCFH-DA was added and incubated with chondrocytes at 37 °C in the dark for 30 min. Relative level of fluorescence in each group was quantified by a multi-functional microplate reader.

2.16. Lipid peroxidation assay

Total proteins in rat chondrocytes were extracted by using the RIPA solution (Beyotime, China). Lysates were processed under ultrasonic and centrifuged at 12,000 g for 5 min. Next, the supernatants were quantified by using the BCA assay. MDA equivalent was examined by using the thiobarbituric acid test as described previously [45].

2.17. Total superoxide dismutase (SOD) activity assay

The SOD activity in each group was detected by using a total SOD Assay Kit with WST-8 (Beyotime, China) [38,46]. First, rat chondrocytes were seeded in a 6-well-plate. After different treatments, the sample preparation solution was added to lyse the chondrocytes. Next, 160 μl WST-8/enzyme working solution and 20 μl chondrocyte lysate supernatant were mixed and added to a 96-well plate, and then 20 μl reaction starter working solution was added into each well and incubated at 37 °C for 30 min. The absorbance in each well was detected at 450 nm by a multi-functional microplate reader.

2.18. Enzyme-linked immunosorbent assay (ELISA)

TNFα, IL6 and MMP13 in culture supernatant were quantified by using ELISA according to the manufacturer's protocol (Abcam, USA). The absorbance in each group was measured at 450 nm by using a multi-functional microplate reader.

2.19. Ethical approval and experimental animals

All SD rats (8-week-old, 250–300 g) were purchased from Sino-British Sippr/BK Lab Animal Ltd (Shanghai, China). Animal experiments were in accordance with the animal care and use committee guidelines and approved by the Animal Research Committee of Shanghai Jiao Tong University Affiliated Sixth People's Hospital (Approval Number: SYXK2016-0020, March 23, 2020, Shanghai, China).

2.20. Monosodium iodoacetate (MIA)-induced rat OA models

In animal studies, SD Rats were randomised and divided into two OA groups (subacute and chronic OA model) and further divided into different treatment groups (n = 10 rats/group). After anaesthesia by isoflurane inhalation, the knee joints of rats received a single intra-articular injection of 3 mg MIA in a volume of 50 μl PBS. The control group were intra-articularly injected with an equivalent volume of PBS. The dose of cell-laden microspheres injected in each treatment group was in terms of the number of microspheres. Firstly, 3 mg microspheres were incubated with 2.5×10^5 CPCs in 500 μl culture medium. After

incubation for 7 days, 100 μl microspheres solution with CPCs were intra-articularly injected into OA rat joint. According to previously published article [47], rats in the subacute OA group were intra-articularly injected with 100 μl hypoxia-pretreated CGMs or normoxia-pretreated CGMs once a week for 28 days before significant OA degeneration (7 days after OA induction). In the chronic OA group, different treatments were given once a week for 56 days after significant OA phenotypes (14 days after OA induction). After 35 days (subacute model) and 70 days (chronic model) of OA induction, rats were sacrificed and the knee joints in each group were harvested for further analyses.

2.21. Histological evaluation

The rat knee joints in all groups were fixed with 4% PFA overnight, decalcified with 10% EDTA for 14 d, embedded in paraffin, and sectioned at 5 μm thickness. Next, the samples were stained to evaluate proteoglycan deposition and cartilage degeneration in each group by using the Alcian Blue Cartilage Staining Kit (Solarbio, China) and Modified Safranin O/fast green Cartilage Staining Kit (Solarbio, China). The Osteoarthritis Research Society International (OARSI) scoring system was also used to assess cartilage degeneration and destruction [48]. The medial tibial bone sclerosis (grade –5–5) was scored by evaluating the subchondral trabecular bone to marrow ratio [49]. Besides, synovial inflammation in each group was scored on an arbitrary scale from 0 to 3 depending on infiltration of inflammatory cells into the synovial membrane by using the Hematoxylin-Eosin (H&E) Staining Kit (Solarbio, China) [49].

2.22. Immunohistochemical (IHC) analysis

For IHC staining, cartilage sections in each group were deparaffinized in xylene, hydrated through ethanol series and repaired by pepsin antigen repair solution (Solarbio, China). Subsequently, cartilage sections were blocked with 5% BSA for 1 h, and incubated with primary antibodies of Collagen II (1:100; Abcam), MMP13 (1:200; Abcam), ADAMTS5 (1:200; Abcam), IL-1β (1:1000; Abcam), IL6 (1:200; Abcam), TNFα (1:200; Cell Signaling Technology), SOD1 (1:200; Abcam), NRF2 (1:100; Abcam), KEAP1 (1:100; Abcam), HO-1 (1:200; Abcam), and NQO1 (1:200; Abcam) at 4 °C overnight before stained with HRP-labeled secondary antibody. Antigen-positive chondrocytes were visualized and analyzed by using the DAB Substrate kit (Servicebio, China).

2.23. OA pain analysis

OA pain in rats was evaluated by the hind-paw withdrawal threshold method according to previous studies [43]. Briefly, rat was placed in an elevated metal grid cage individually with enough space to move its paws, while the rest body was restricted with plastic plate. After acclimated to the apparatus for 7 d, right hind-paw withdrawal threshold of each rat was detected by using the electronic von Frey instrument (BIO-EVF4; Bioseb, Vitrolles France). First, the probe tip was gently placed perpendicularly into the mid-plantar surface of the paw. Next, increasing pressure (0–100 g) was applied until the rat hind paw was first lifted, and this force is independent of the movements of the limb. The hind-paw withdrawal threshold (g) was recorded as the required pressure to first lift the rat paw. Lower withdrawal threshold values (g) were taken as indicators of OA pain.

2.24. Statistical analysis

Statistical analysis was processed by GraphPad prism 8.0. Quantitative results were presented as mean ± standard deviation (S.D.) values. The Student's t-test was applied for comparison between two groups. One-way analysis of variance (ANOVA) was performed for comparisons among various groups. All experiments were repeated at least three times independently and representative experiment data are presented.

Significant difference was defined as $P < 0.001$ (***, ###), $P < 0.01$ (**, ##), and $P < 0.05$ (*, #).

3. Results

3.1. The proliferative and chondrogenic ability of 2D or 3D cultured CPCs under normoxic and hypoxic conditions

First, the GelMA Crosslinked Microspheres (GMs) were constructed and characterized by SEM. The SEM images showed GMs are transparent regular spheroids and the diameter of GMs is about 100 nm (Fig. S1). For another, CPCs were obtained from superficial articular cartilage of rat femoral head. The morphology of CPCs was observed by using a microscopy and we found typical colony formation after primary CPCs culture for 12 days (Fig. S2A). CPCs displayed a small, round or polygonal morphology, and the cells arranged in whorls or bundles (Fig. S2A). Immunofluorescence staining indicated the cells highly expressed CPCs specific markers CD105 and PRX1 (Fig. S2B). In addition, the CPCs expressed cell surface biomarkers that are found on the stem cells typically. The flow cytometry analysis demonstrated that CPCs were homogeneously positive for CD29 (97.62%), CD44 (78.14%), CD105 (67.63%) and CD90 (45.25%) (Fig. S3A), which were comparable with those in the MSCs (CD29, 99.90%; CD44, 80.70%; CD105, 98.90%; and CD90, 84.08%) (Fig. S3B) and articular chondrocytes (CD29, 93.27%; CD44, 0.31%; CD105, 4.67%; and CD90, 0.05%) (Fig. S3C). For another, CPCs were negative for CD45 (0.10%) and CD146 (0.10%) (Fig. S3).

Then, CPCs were cultured with GMs under normoxic or hypoxic culture condition to evaluate their proliferative ability and chondrogenic capacity (Fig. 1A). The result of CCK8 assay demonstrated that the number of 3D cultured CPCs under hypoxic condition was significantly higher than that of 2D cultured CPCs and 3D cultured CPCs under normoxic condition (Fig. 1B). Next, the cartilage matrix GAG and collagen contents were detected after chondrogenic induction. We found the cartilage matrix GAG content in hypoxia-pretreated CGMs group was significantly higher than the normoxia-pretreated CGMs group (Fig. 1C), indicating the successful generation of much cartilage matrix in hypoxia-preconditioned CGMs. Our results also showed hypoxia-preconditioned CGMs produced more collagen content than 2D cultured CPCs (Fig. 1D). PCR analysis revealed that the hypoxia-preconditioned CGMs up-regulated the expression of cartilage matrix gene *Acan* and *Col2a1* when compared with the 2D cultured CPCs and normoxia-pretreated CGM groups (Fig. 1E and F). To evaluate the chondrogenic capacity of hypoxia-pretreated CGMs, the mRNA expressions of cartilage superficial zone gene *Prp4* (also known as lubricin), chondrogenic genes *Gdf5*, *Sox6*, and *Sox9* were detected by PCR analysis. Our results showed hypoxia-pretreated CGMs expressed the highest levels of classical chondrogenic genes *Gdf5*, *Prp4*, *Sox6*, and *Sox9*, compared to the normoxia-pretreated CGMs group and other groups (Fig. 1G–J). Western blot analysis showed similar results as PCR analysis and we found hypo-CGMs more effectively promoted the protein expressions of anabolism-related markers (Collagen II, GDF5, PRG4, SOX9) than the norm-CGMs group (Fig. S6). Additionally, we further detected the cell viability and chondrogenic

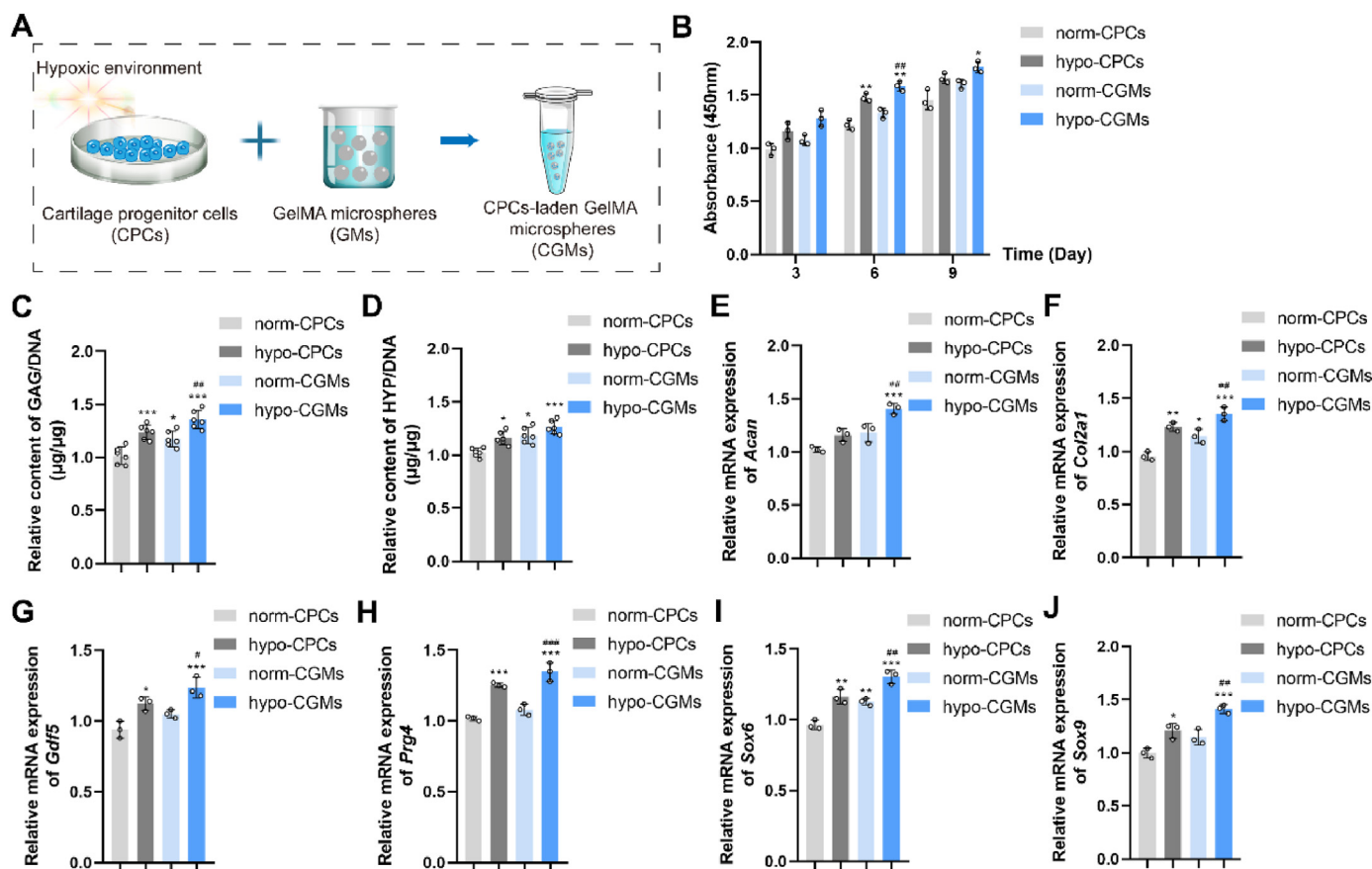


Fig. 1. The chondrogenic capacity of 3D cultured CPCs under normoxic and hypoxic conditions. (A) Construction of 3D cultured CPCs using gelatin methacryloyl (GelMA) microspheres (GMs) under hypoxic condition. (B) Cell proliferative ability of CPCs was detected after incubation for different time points (3 d, 6 d, 9 d) by CCK8 assay ($n = 3$). (C) Relative matrix GAG content was detected in each group after incubation for 7 days ($n = 6$). (D) Relative matrix collagen content was analyzed after induction under different conditions for 7 days ($n = 6$). (E and F) The mRNA expressions of anabolism-related genes (*Acan* and *Col2a1*) in each group were assessed after incubation for 7 days by PCR analysis ($n = 3$). (G–H) The mRNA expressions of chondrogenic genes (*Gdf5*, *Prp4*, *Sox6*, and *Sox9*) in each group were assessed after incubation for 7 days by PCR analysis ($n = 3$). Data represent mean \pm S.D. * $P < 0.05$, ** $P < 0.01$, *** $P < 0.001$ versus the norm-CPCs group. # $P < 0.05$, ## $P < 0.01$, ### $P < 0.001$ versus the norm-CGMs group.

ability of CGMs under normoxic or hypoxic condition for a 28-d period. Our results showed the cell viability of CPCs showed no significant difference after incubation for 14 days under normoxic or hypoxic condition (Fig. S4). PCR results demonstrated that the expressions of chondrogenic genes showed no obvious difference after 21 days incubation under normoxic or hypoxic condition (Fig. S5). Altogether, our results suggest that 3D cultured CPCs under hypoxic environment exhibit stronger proliferative ability and chondrogenic capacity as compared to that of 2D culture condition and normoxic environment.

3.2. The chondro-protective effects of 3D cultured CPCs under normoxic and hypoxic conditions

Next, we further evaluated the chondro-protective effects of 3D cultured CPCs under normoxic and hypoxic environment in IL-1 β -activated chondrocytes by using the indirect-coculture system (Fig. 2A). First, chondrocytes were treated with different concentrations of IL-1 β and our results showed that chondrocyte viability was apparently reduced after IL-1 β treatment compared with that of the control group

from 5 ng/ml to 25 ng/ml (Fig. S7). Finally, 10 ng/ml of IL-1 β was chosen to induce OA phenotypes in chondrocytes. The results of CCK8 assay also showed proliferative ability was obviously inhibited in IL-1 β -induced chondrocytes, while coculture with hypoxia-pretreated CGMs effectively reversed this condition and normoxia-pretreated CGMs had no significant effect on promoting the proliferation of IL-1 β -activated chondrocytes (Fig. 2B). Then, we evaluated the effects of hypoxia-pretreated CGMs on cartilage matrix metabolism in IL-1 β -activated chondrocytes. Compared to 3D cultured CPCs under normoxic condition, coculture with 3D cultured CPCs under hypoxic environment showed a stronger deposition of GAG in IL-1 β -activated chondrocytes (Fig. 2C). Moreover, our results also demonstrated hypoxia-pretreated CGMs significantly increased the collagen content in IL-1 β -activated chondrocytes, while normoxia-pretreated CGMs had no significant effect on promoting the production of collagen (Fig. 2D). PCR analysis revealed that coculture with hypoxia-pretreated CGMs more effectively up-regulated the mRNA expressions of cartilage matrix anabolism genes (*Acan*, *Col2a1*, and *Prg4*) (Fig. 2E–G) and down-regulated the mRNA expressions of catabolism genes (*Adams5*, *Mmp3*, and *Mmp13*) (Fig. 2H–J), compared with the

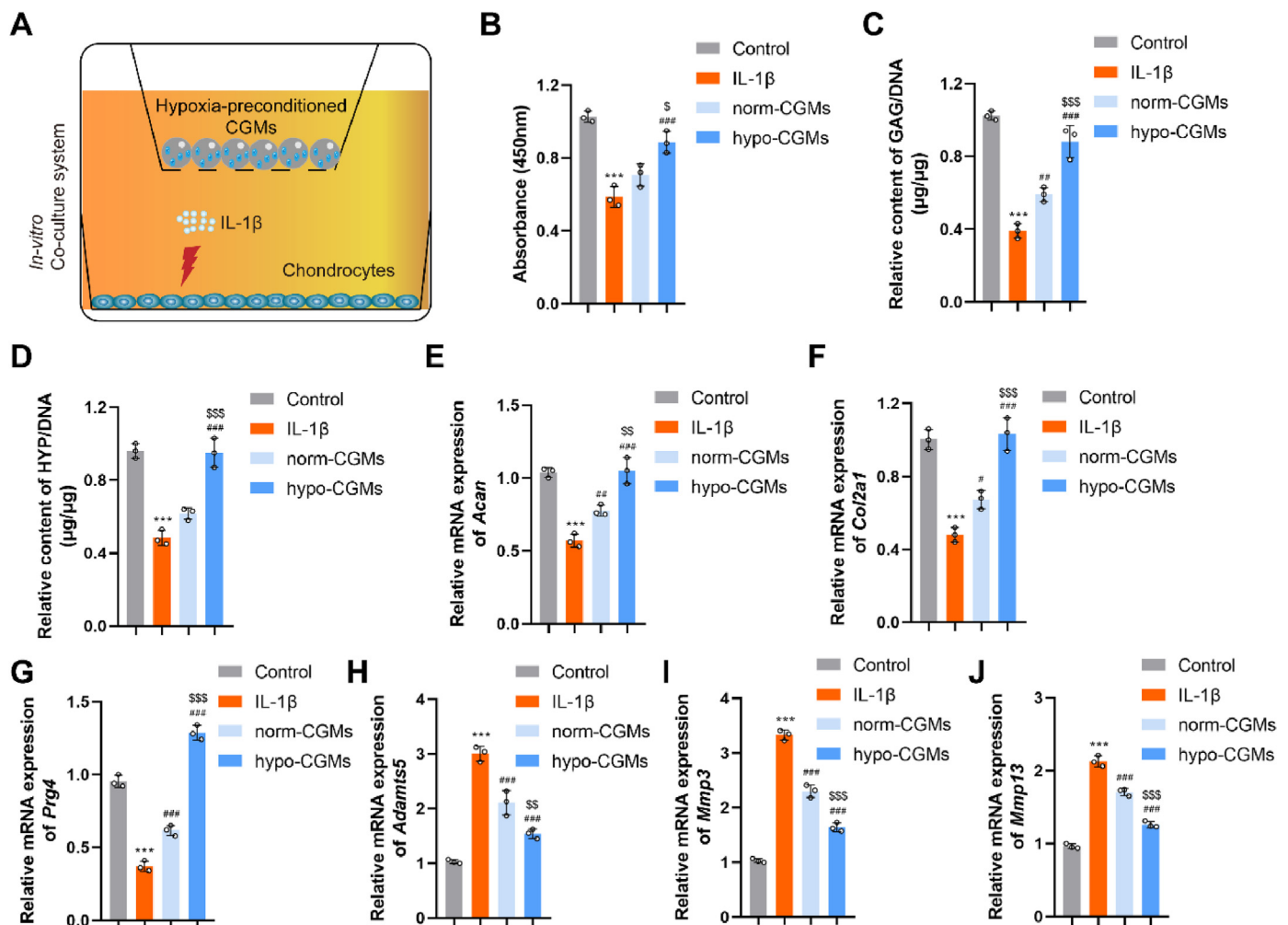


Fig. 2. Hypoxia-pretreated CGMs promote cell proliferation and maintain matrix metabolism balance in IL-1 β -induced chondrocytes. (A) A transwell co-culture system was applied for exploring the chondro-protective effects of CGMs in IL-1 β -induced chondrocytes. (B) Chondrocyte proliferative ability in each group was detected after co-incubation for 48 h by CCK8 assay (n = 3). (C) Relative matrix GAG content was detected after co-incubation for 48 h in different groups (n = 3). (D) Relative matrix collagen content was analyzed after co-incubation for 48 h in each group (n = 3). (E and F) Relative mRNA expressions of anabolism-related genes (*Acan* and *Col2a1*) were evaluated after co-incubation for 48 h by PCR analysis (n = 3). (G) The mRNA expression of chondrogenic gene *Prg4* was detected after co-incubation for 48 h by PCR analysis (n = 3). (H–J) Relative mRNA expressions of catabolism-related genes (*Adams5*, *Mmp3*, and *Mmp13*) were detected after co-incubation for 48 h by PCR analysis (n = 3). Data represent mean \pm S.D. ***P < 0.001 versus the Control group. #P < 0.05, ##P < 0.01, ###P < 0.001 versus the IL-1 β group. $^{\$}$ P < 0.05, $^{\$\$}$ P < 0.01, $^{\$ \$ \$}$ P < 0.001 versus the norm-CGMs group.

normoxia-pretreated CGMs group. Consistent with PCR results, western blot analysis also demonstrated that hypo-CGMs more effectively promoted the protein expressions of anabolism-related markers (Aggrecan, Collagen II, PRG4) and inhibited the protein expression of catabolism-related marker (ADAMTS5) in IL-1 β -induced chondrocytes than norm-CGMs (Fig. S8). Together, our results demonstrated that 3D cultured CPCs under hypoxic condition showed strong proliferative ability and anti-catabolism effect in IL-1 β -activated chondrocytes.

3.3. Hypoxia-pretreated CGMs inhibit oxidative stress and inflammation in IL-1 β -induced chondrocytes via NRF2/HO-1 pathway

In the following part, we further assessed the effects of 3D cultured CPCs on IL-1 β -activated oxidative stress and inflammatory activity in chondrocytes. First, to explore whether oxidative stress was associated with the protective effect of 3D cultured CPCs, the levels of MDA, ROS, and SOD were detected. After coculture with hypoxia-pretreated CGMs, we observed a more significant down-regulation in the level of MDA in IL-1 β -activated chondrocytes, compared to normoxia-pretreated CGMs group (Fig. 3A). Our results also showed coculture with hypoxia-pretreated CGMs significantly decreased the production of ROS in IL-1 β -activated chondrocytes, while normoxia-pretreated had no obvious inhibitory effect on ROS production (Fig. 3B). In addition, hypoxia-pretreated CGMs obviously increased the activity of anti-oxidant enzyme SOD in IL-1 β -activated chondrocytes, but normoxia-pretreated CGMs showed no significant effect on promoting the level of SOD in IL-1 β -activated chondrocytes (Fig. 3C). These results confirmed that hypoxia-pretreated CGMs exhibited significant anti-oxidant effect in IL-1 β -activated chondrocytes. Then we investigated the anti-inflammation effect of 3D cultured CPCs in IL-1 β -activated chondrocytes. Compared with the control group, the ELISA assay results demonstrated that IL-1 β significantly increased the production of inflammatory factors (TNF α , IL6, and MMP13) in chondrocytes, while hypoxia-pretreated CGMs effectively down-regulated the levels of these inflammatory factors (Fig. 3D). Additionally, our results of PCR analysis further confirmed that hypoxia-pretreated CGMs more effectively decreased the mRNA expressions of inflammatory factors (*Tnf α* , *Il6*, *iNOS*, and *Cox2*) (Fig. 3E–H) and up-regulated the mRNA levels of anti-oxidant enzymes (*Sod1* and *Sod2*) (Fig. 3I and J), compared with the norm-CGMs group. Together, these results suggested that coculture with 3D cultured CPCs under hypoxic condition showed a stronger anti-oxidative stress and anti-inflammation ability than normoxia-pretreated 3D cultured CPCs in IL-1 β -activated chondrocytes.

To better understand the potential mechanism of the anti-oxidative stress and anti-inflammatory effect of hypoxia-pretreated CGMs on IL-1 β -activated chondrocytes, the role of classic NRF2/HO-1 pathway was investigated in the following study. PCR analysis showed hypoxia-pretreated CGMs up-regulated the mRNA expressions of NRF2 as well as its downstream HO-1 and NADPH quinone oxidoreductase 1 (NQO1) (Fig. 3K). Western blot analysis also demonstrated a similar result with PCR analysis, 3D cultured CPCs under hypoxic condition significantly promoted the protein expressions of NRF2 and HO-1 in IL-1 β -activated chondrocytes (Fig. 3L and Fig. S9). Immunofluorescence staining for NRF2 showed that hypo-CGMs treatment led to significant nuclear translocation of NRF2, while norm-CGMs showed no obvious difference (Fig. S10).

Furthermore, a classical NRF2 inhibitor 40 nM brusatol was co-treated with CGMs on chondrocytes. Our results showed that brusatol significantly inhibited the expression of NRF2 and downstream proteins (Fig. S11C and D). We also found that brusatol abrogated the chondro-protective effects of hypo-CGMs and the protein expressions of ADAMTS5, TNF α , and IL6 were up-regulated (Fig. S11A and B). Overall, our findings indicated that 3D cultured CPCs under hypoxic condition probably attenuated oxidative stress and inflammation in IL-1 β -activated chondrocytes by activating the NRF2/HO-1 pathway.

3.4. Hypoxia-pretreated CGMs attenuate cartilage degeneration and promote matrix anabolism in MIA-induced subacute OA rat

In consideration of the chondro-protective effects of hypoxia-pretreated CGMs *in vitro*, we further investigated whether hypoxia-pretreated CGMs could exert a strong chondro-protective effects in subacute rat OA model. Seven days after MIA injection, different treatments were intra-articularly injected into the knee joint once a week (Fig. 4A). After different treatments for four weeks, hypoxia-pretreated CGMs effectively attenuated cartilage destruction and promoted matrix anabolism in subacute OA rat (Fig. 4B). The OARSI score in OA rat was significantly declined from 4.20 ± 0.75 to 1.80 ± 0.75 ($P = 0.0003$) after hypoxia-pretreated CGMs treatment, compared to the PBS-treated group (Fig. 4C). Additionally, hypo-CGMs more effectively decreased the OARSI score than the norm-CGMs group (Fig. 4C). Our results also showed that hypoxia-pretreated CGMs decreased the osteophyte maturity 2.40 ± 0.80 to 1.40 ± 0.49 ($P = 0.57$) in OA rat (Fig. 4D). Moreover, the medial tibial bone score in OA rat was down-regulated from 3.00 ± 0.63 to 1.60 ± 0.80 ($P = 0.0993$) after the intervention of hypoxia-pretreated CGMs, compared to the PBS-treated group (Fig. 4E). Besides, the IHC analysis was carried out to evaluate the expressions of anabolism-related marker Collagen II and catabolism-related marker MMP13 and ADAMTS5 in articular cartilage of rat (Fig. 4F). The decreased expression of Collagen II in cartilage was reversed by hypoxia-pretreated CGMs. In addition, compared to the normoxia-pretreated CGMs-treated group, hypoxia-pretreated CGMs effectively down-regulated the levels of MMP13 and ADAMTS5 (Fig. 4G and H). These results indicated that hypoxia-pretreated CGMs successfully ameliorated cartilage destruction and maintained matrix metabolism balance in subacute OA rat.

3.5. Hypoxia-pretreated CGMs suppress inflammation and oxidative stress by activating NRF2/HO-1 pathway in MIA-induced subacute OA rat

To investigate whether oxidative stress and inflammation were involved in hypoxia-pretreated CGMs-mediated cartilage protection *in vivo*, we evaluated the anti-oxidant and anti-inflammatory effects of hypoxia-pretreated CGMs in articular cartilage of subacute OA rat model. H&E staining indicated hypoxia-pretreated CGMs attenuated the infiltration of inflammatory cells in synovium (Fig. 5A), and the inflammation score was decreased from 2.00 ± 0.63 to 1.00 ± 0.63 ($P = 0.1455$) after hypoxia-pretreated CGMs treatment, compared to the PBS-injected group (Fig. 5B). In addition, our results showed hypoxia-pretreated CGMs effectively up-regulated the withdrawal threshold (from 42.80 ± 6.55 g to 69.80 ± 8.86 g), compared with the PBS-treated group (Fig. S3). IHC staining for inflammatory factors verified that hypoxia-pretreated CGMs and normoxia-pretreated CGMs both down-regulated the expressions of IL-1 β , IL6, and TNF α , while hypoxia-pretreated CGMs more effectively decreased the ratio of IL6-positive and TNF α -positive chondrocytes than normoxia-pretreated CGMs (Fig. 5C–F). Moreover, IHC analysis also confirmed that hypoxia-pretreated CGMs obviously increased the expression of anti-oxidant enzyme SOD1 in OA rat (Fig. 5G and H). Together, our results indicated hypoxia-pretreated CGMs exert stronger chondro-protective effects than normoxia-pretreated CGMs in subacute OA rat.

To further explore whether the NRF2/HO-1 pathway played an essential role in the anti-oxidant and anti-inflammatory effects of hypoxia-pretreated CGMs *in vivo*, we further detected the expressions of NRF2, KEAP1, HO-1, and NQO1 by IHC staining. IHC analysis results demonstrated that normoxia-pretreated and hypoxia-pretreated CGMs both significantly up-regulated the expressions of NRF2 (Fig. 5J) and KEAP1 (Fig. S12A and B) as well as downstream targets HO-1 and NQO1 (Fig. 5J and K). Besides, we found hypo-CGMs more effectively down-regulated the number of NRF2-positive and KEAP1-positive chondrocytes than norm-CGMs group in subacute OA rat

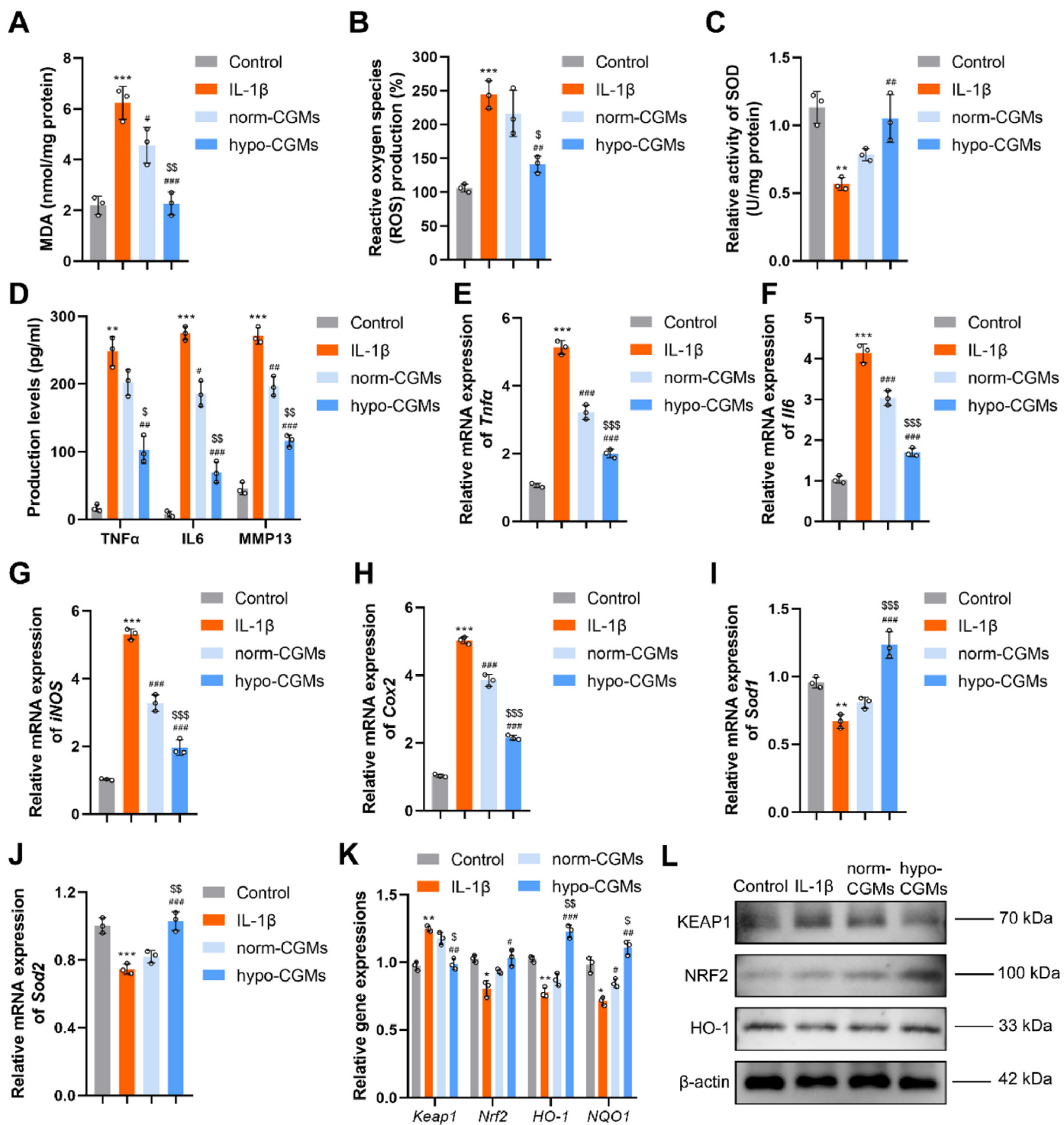


Fig. 3. Hypoxia-pretreated CGMs alleviate oxidative stress and inflammatory response and promote NRF2/HO-1 pathway activation in IL-1β-induced chondrocytes. (A) The level of malondialdehyde (MDA) in each group was detected after co-incubation for 48 h (n = 3). (B) The levels of reactive oxygen species (ROS) in different groups were analyzed after co-incubation for 48 h (n = 3). (C) Superoxide dismutase (SOD) activity levels were evaluated after different treatments after co-incubation for 48 h (n = 3). (D) The concentrations of TNFα, IL6, and MMP13 were evaluated after co-incubation for 48 h by ELISA assay (n = 3). (E–H) The mRNA expressions of the inflammatory factors (*Tnfa*, *Il6*, *iNOS*, and *Cox2*) in each group were detected after co-incubation for 48 h by PCR analysis (n = 3). (I and J) The mRNA expressions of the antioxidant genes (*Sod1* and *Sod2*) were detected after co-incubation for 48 h by PCR analysis (n = 3). (K) The mRNA expressions of the NRF2/HO-1 pathway-related genes (*Keap1*, *Nrf2*, *HO-1*, and *NQO1*) were detected after co-incubation for 48 h by PCR analysis (n = 3). (L) The protein expressions of the NRF2/HO-1 pathway-related markers (KEAP1, NRF2, and HO-1) were assessed after co-incubation for 48 h by western blotting analysis. Data represent mean ± S.D. *P < 0.05, **P < 0.01, ***P < 0.001 versus the Control group. #P < 0.05, ##P < 0.01, ###P < 0.001 versus the IL-1β group. \$P < 0.05, \$\$P < 0.01, \$\$\$P < 0.001 versus the norm-CGMs group.

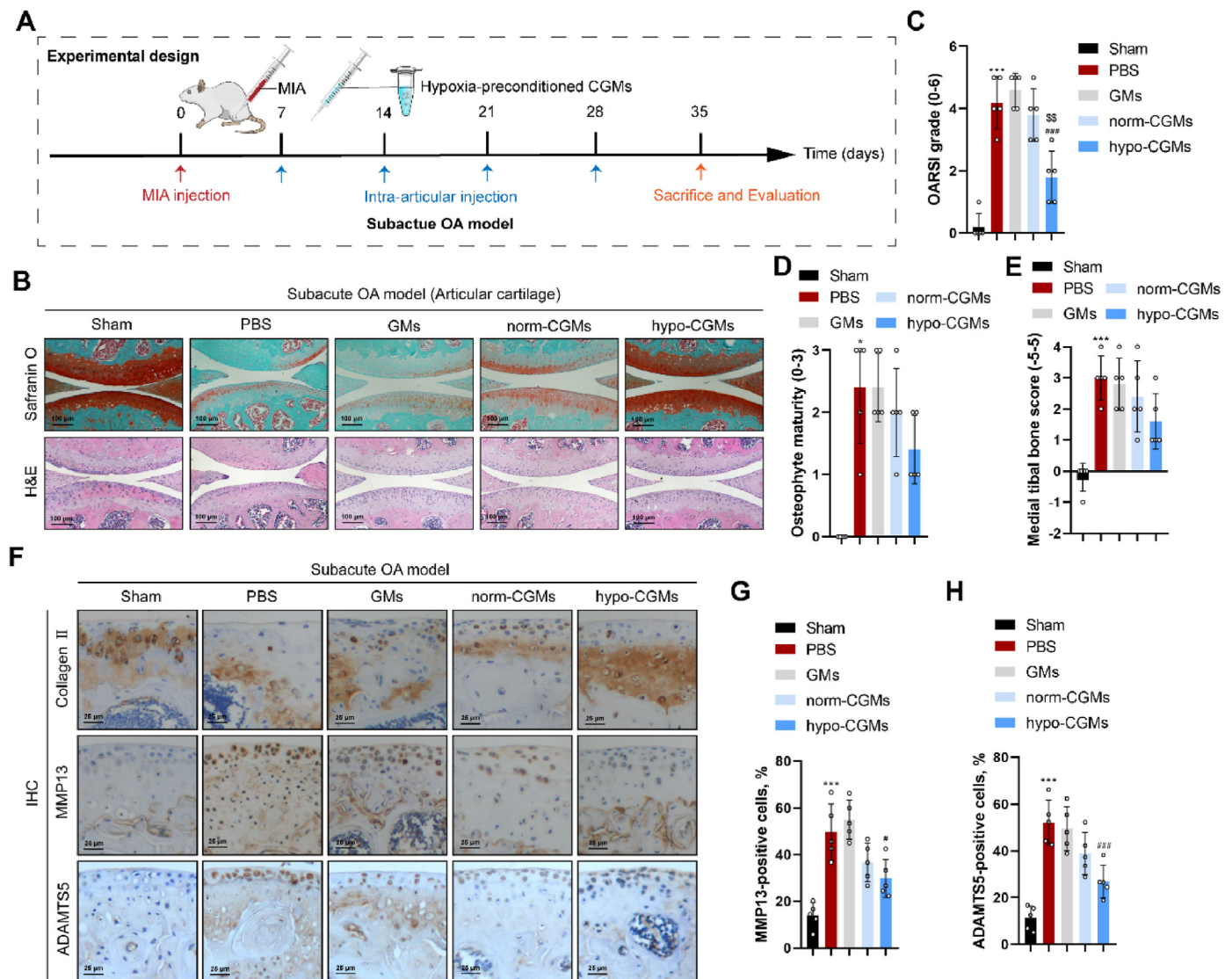


Fig. 4. Hypoxia-pretreated CGMs attenuate cartilage degeneration and matrix catabolism in subacute OA rat. (A) Schematic of the time course for the experiments in MIA-induced subacute OA rat. OA rats were intra-articularly injected with different treatments and evaluated as indicated. (B) Representative micrographs of Safranin O staining and H&E staining after different treatments. Scale bar, 100 μ m. (C) The OA severity in each group was measured by the Osteoarthritis Research Society International (OARSI) scoring system (n = 5). (D) Osteophyte formation in each group was determined and scored (n = 5). (E) The score of medial tibial bone in each group was evaluated (n = 5). (F) Representative micrographs of immunohistochemical staining for Collagen II, MMP13, and ADAMTS5 after different treatments. Scale bar, 25 μ m. (G and H) Quantification of MMP13-positive and ADAMTS5-positive chondrocytes after different treatments in subacute OA rat (n = 5). Data represent mean \pm S.D. *P < 0.05, ***P < 0.001 versus the Sham group. #P < 0.05, ###P < 0.001 versus the PBS group. \$P < 0.01 versus the norm-CGMs group.

(Fig. 5I and Fig. S12A-B). Accordingly, 3D cultured CPCs under hypoxic condition effectively ameliorated cartilage degeneration and maintained cartilage matrix metabolism balance by inhibiting oxidative stress and inflammation via activation of NRF2/HO-1 pathway in subacute rat OA model.

3.6. Hypoxia-pretreated CGMs rescue cartilage degradation and maintain matrix metabolism balance in chronic OA rat

To comprehensively assess the *in vivo* therapeutic effect of hypoxia-pretreated CGMs for OA, we further constructed a MIA-induced chronic rat model. Different treatments were intra-articularly injected into the knee joint of rat once a week for eight weeks (Fig. 6A). The damage of articular cartilage and loss of proteoglycan were obviously detected in MIA-induced rat by using H&E and Safranin O staining, while hypoxia-pretreated CGMs ameliorated cartilage degeneration (Fig. 6B). Meanwhile, our results also revealed that hypoxia-pretreated CGMs more

effectively down-regulated the OARSI score in PBS-treated OA rat (from 4.80 ± 0.98 to 2.00 ± 0.63) than the norm-CGMs group, and there was no significant difference ($P = 0.75$) between normoxia-pretreated CGMs-treated group and PBS-treated group (Fig. 6C). Our result also demonstrated that hypoxia-pretreated CGMs effectively decreased the osteophyte maturity from 2.80 ± 0.40 to 1.40 ± 0.49 in OA rat, but normoxia-pretreated CGMs had no significant regulatory effect ($P = 0.14$) on osteophyte maturity (Fig. 6D). In addition, the medial tibial score was declined from 3.20 ± 0.75 to 1.80 ± 0.75 in PBS-treated rat after the treatment of hypoxia-pretreated CGMs (Fig. 6E). Moreover, the expression of Collagen II was increased in hypoxia-pretreated CGMs-treated group compared to that of PBS-treated group, which is consistent with the results in subacute OA rat model (Fig. 6F). IHC analysis results showed that hypoxia-pretreated CGMs significantly decreased the number of MMP13-positive and ADAMTS5-positive chondrocytes in chronic OA rat (Fig. 6G and H). The above results indicated 3D cultured CPCs under hypoxic condition exhibited a

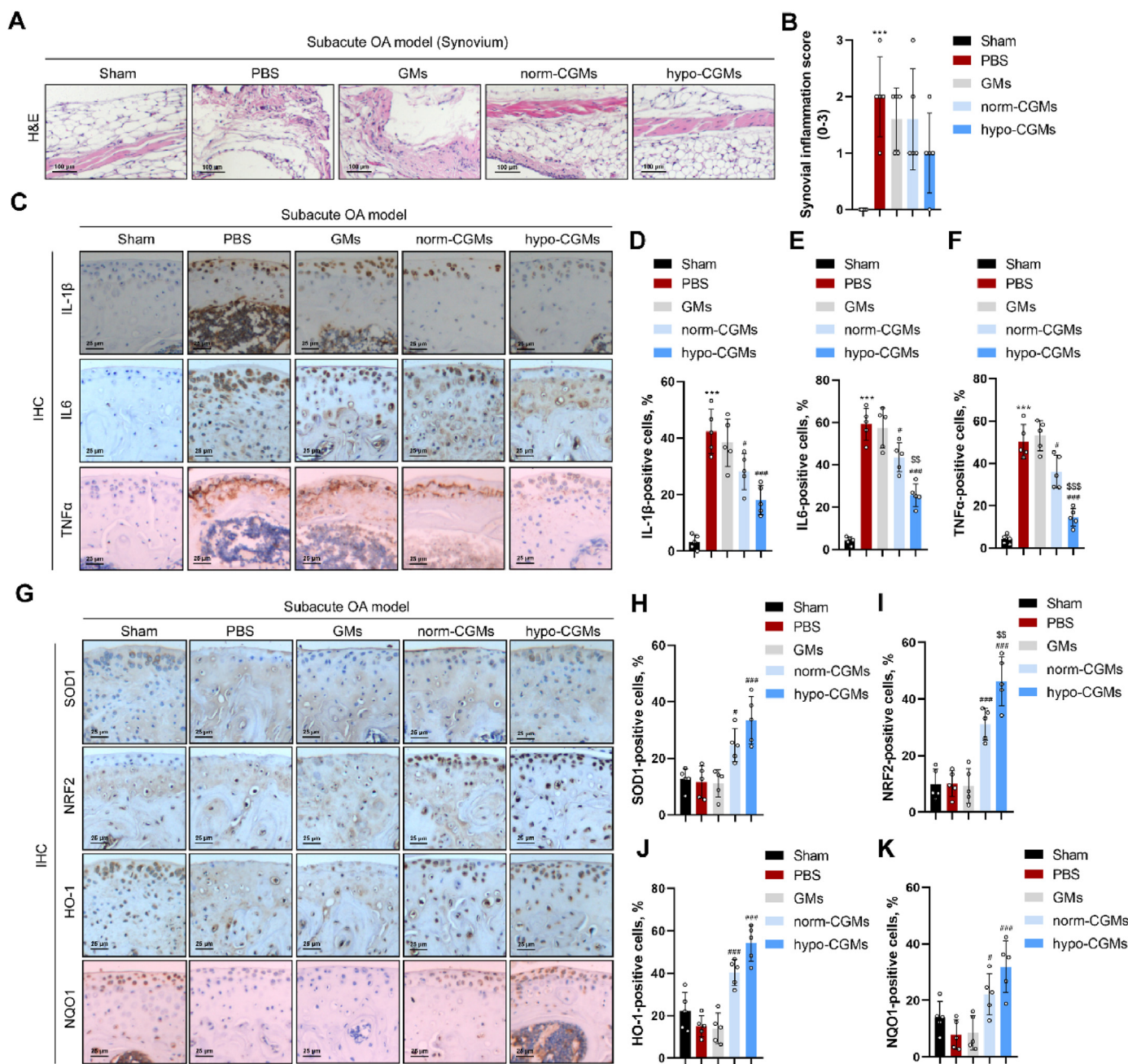


Fig. 5. Hypoxia-pretreated CGMs ameliorate cartilage inflammatory response and oxidative stress and activate NRF2/HO-1 pathway in subacute OA rat. (A and B) Synovial inflammation in each group was determined by H&E staining and scored (n = 5). (C) Immunohistochemical staining inflammatory factors (IL-1β, IL6, and TNFα) in different groups (n = 5). Scale bar, 25 μm. (D–F) Quantification of IL-1β-positivity, IL6-positivity, and TNFα-positivity in chondrocytes after different treatments in subacute OA rat (n = 5). (G) Immunohistochemical staining of antioxidant enzyme SOD1 and the NRF2/HO-1 pathway-associated markers (NRF2, HO-1, and NQO1) in different groups (n = 5). Scale bar, 25 μm. (H) Quantification of SOD1-positive chondrocytes after different treatments (n = 5). (I–K) Quantification of NRF2-positivity, HO-1-positivity, and NQO1-positivity in chondrocytes in different groups (n = 5). Data represent mean ± S.D. ***P < 0.001 versus the Sham group. #P < 0.05, ###P < 0.001 versus the PBS group. ^{SS}P < 0.01, ^{SSS}P < 0.001 versus the norm-CGMs group.

significant cartilage protective effect in chronic OA rat model.

3.7. Hypoxia-pretreated CGMs ameliorate inflammation and oxidative stress through activating NRF2/HO-1 pathway in chronic OA rat

In addition to cartilage degeneration and matrix metabolism, we further evaluated the anti-inflammatory and anti-oxidant effects in chronic OA rat after treatments. The results of H&E staining demonstrated that hypoxia-pretreated CGMs ameliorated inflammatory response in synovium (Fig. 7A), and the synovial inflammation score was declined from 2.20 ± 0.40 to 1.00 ± 0.63, compared to the PBS-treated

group (Fig. 7B). Additionally, hypoxia-pretreated CGMs obviously relieved OA-related pain as withdrawal threshold was raised from 45.40 ± 5.68 g to 63.20 ± 7.36 g (Fig. S4), compared to the PBS-treated group. Meanwhile, compared to the PBS-treated group (45.40 ± 5.68 g), an up-regulation of withdrawal threshold was observed in the normoxia-pretreated CGMs-treated group (54.00 ± 6.60 g), but there is no significant difference between PBS-treated group and normoxia-pretreated CGMs-treated group (P = 0.36) (Fig. S4). IHC staining for inflammatory factors in articular cartilage showed that hypoxia-pretreated CGMs markedly decreased the expressions of IL-1β, IL6, and TNFα in chronic OA rat (Fig. 7C–F). IHC analysis also demonstrated that hypoxia-

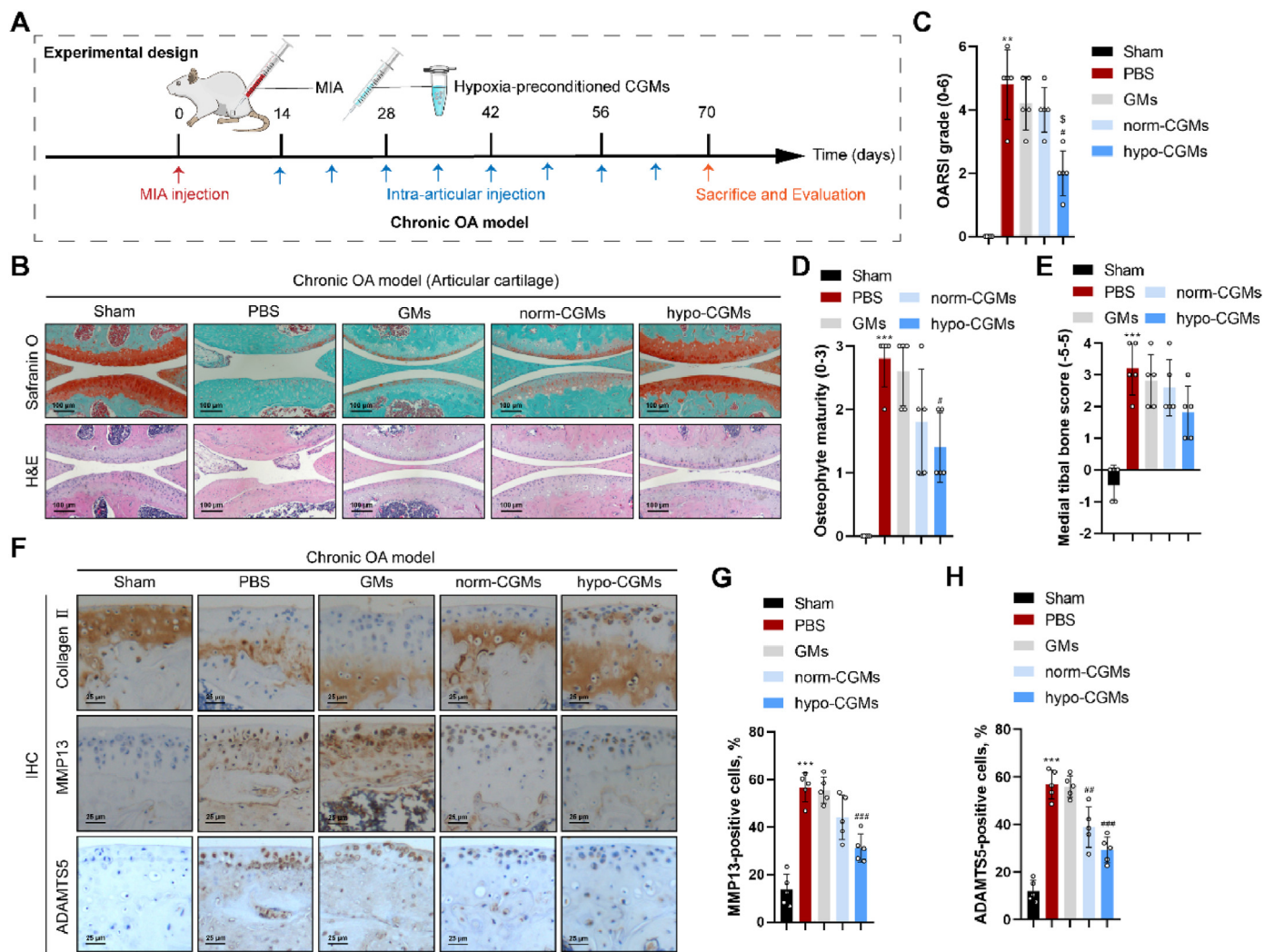


Fig. 6. Hypoxia-pretreated CGMs attenuate cartilage destruction and maintain matrix metabolism balance in chronic OA rat. (A) Schematic of the time course for the experiments in MIA-induced chronic OA rat. OA rats were intra-articularly injected with different treatments and evaluated as indicated. (B) Safranin O staining and H&E staining were performed in each group to assess the level of cartilage degeneration. Scale bar, 100 μ m. (C) The OA severity was measured by the Osteoarthritis Research Society International (OARSIS) scoring system ($n = 5$). (D) Osteophyte formation in each group was determined and scored ($n = 5$). (E) The score of medial tibial bone in each group was evaluated ($n = 5$). (F) Representative micrographs of immunohistochemical staining for Collagen II, MMP13, and ADAMTS5 after different treatments. Scale bar, 25 μ m. (G and H) Quantification of MMP13-positive and ADAMTS5-positive chondrocytes in each group ($n = 5$). Data represent mean \pm S.D. ** $P < 0.01$, *** $P < 0.001$ versus the Sham group. # $P < 0.05$, ## $P < 0.01$, ### $P < 0.001$ versus the PBS group. $^{\$}P < 0.05$ versus the norm-CGMs group.

pretreated CGMs effectively increased the number of SOD1-positive chondrocytes in articular cartilage of chronic OA rat, while normoxia-pretreated CGMs group showed no significant difference compared with the PBS-treated group (Fig. 7H). These results suggested that hypoxia-pretreated CGMs more effectively inhibit oxidative stress in chronic OA rat than normoxia-pretreated CGMs group.

Mechanistically, our IHC staining results showed that hypoxia-pretreated CGMs and normoxia-pretreated CGMs both markedly up-regulated the expressions of NRF2 and KEAP1 (Fig. 7I and Fig. S12C-D) and downstream targets HO-1 and NQO1 (Fig. 7J and K) in chronic OA rat. Our results also demonstrated that hypoxia-pretreated CGMs more effectively up-regulated the ratio of NRF2-positive chondrocytes in chronic OA rat than normoxia-pretreated CGMs (Fig. 7I). Altogether, our findings demonstrated that 3D cultured CPCs under hypoxic environment effectively exerted chondro-protective effects by activating the NRF2/HO-1 signaling pathway in chronic rat OA model.

4. Discussion

OA is a common degenerative joint disease that mainly affects

articular cartilage, characterized by an imbalance between cartilage matrix anabolism and catabolism. Currently, there is no effective pharmacological treatment to restore the morphology of articular cartilage or prevent the loss of cartilage matrix in clinic [1,5]. In this work, an injectable hypoxia-pretreated 3D cultured CPCs delivery system was constructed with the aim to orchestrate chondrogenic microenvironment in the joint for OA cartilage repair and regeneration. Our *in vitro* studies demonstrated that hypoxia-pretreated CGMs significantly promote chondrocyte proliferation and maintain cartilage matrix metabolism balance. Our results also showed hypoxia-pretreated CGMs alleviated cartilage degeneration and promote matrix anabolism by inhibiting oxidative stress and inflammation in both subacute and chronic OA rat models. Additionally, the NRF2/HO-1 pathway played an important part in the chondro-protective effects of hypoxia-pretreated CGMs *in vitro* and *in vivo*. Thus, these findings suggest that the hypoxia-pretreated 3D cultured CPCs delivery system provides an efficient strategy for OA treatment in clinical application.

Stem cells-based therapy is emerging as a promising treatment to promote the repair of injured and damaged tissues in regenerative medicine. Owing to their self-renewal ability and chondrogenic

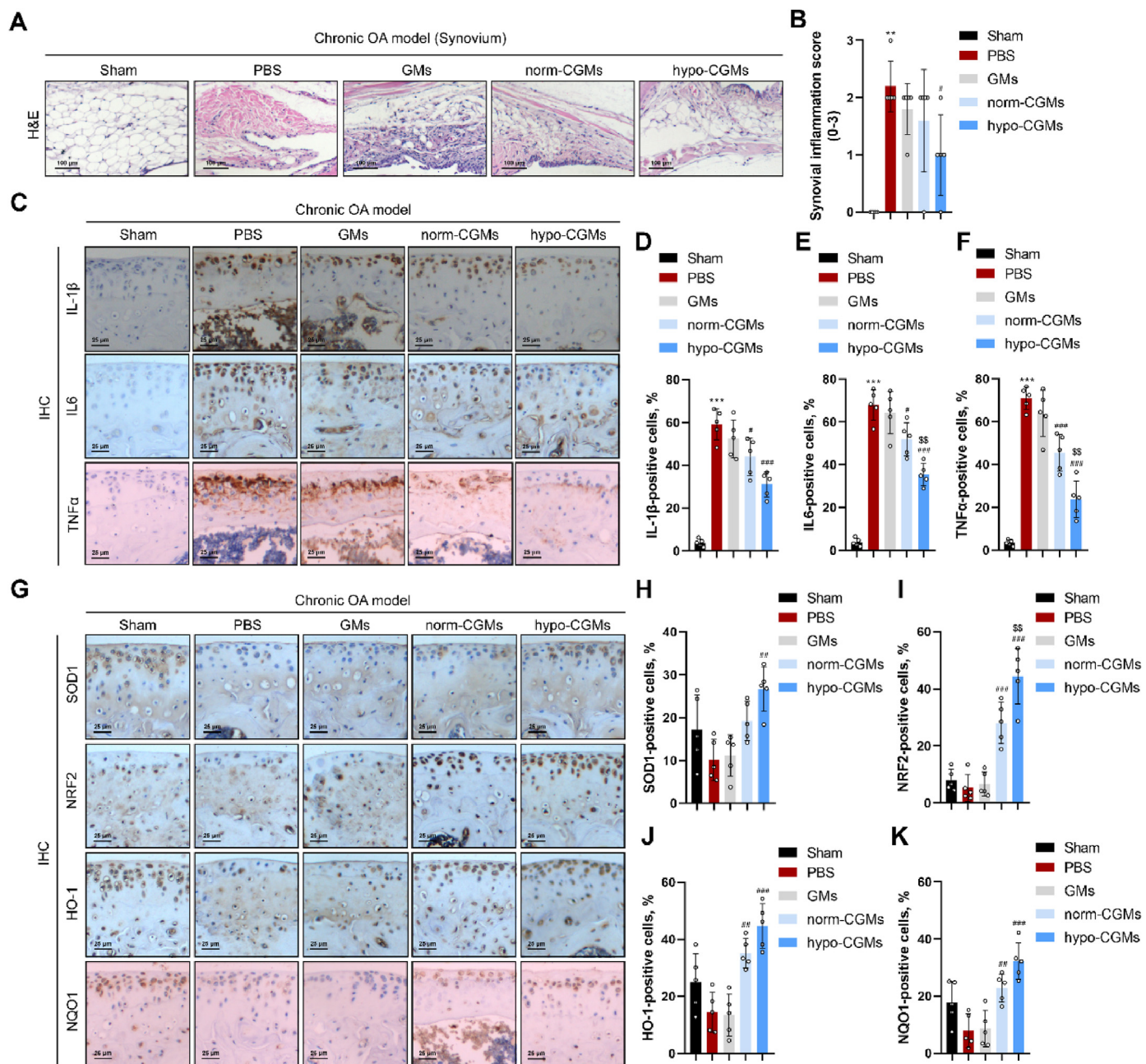


Fig. 7. Hypoxia-pretreated CGMs alleviate cartilage inflammation and oxidative stress and promote the activation of NRF2/HO-1 pathway in chronic OA rat. (A and B) Synovial inflammation in each group was determined by H&E staining and scored (n = 5). (C) Immunohistochemical staining inflammatory factors (IL-1β, IL6, and TNFα) in articular cartilage (n = 5). Scale bar, 25 μm. (D-F) Quantification of IL-1β-positivity, IL6-positivity, and TNFα-positivity in chondrocytes after different treatments in chronic OA rat (n = 5). (G) Immunohistochemical staining of antioxidant enzyme SOD1 and the NRF2/HO-1 pathway-related markers (NRF2, HO-1, and NQO1) in different groups (n = 5). Scale bar, 25 μm. (H) Quantification of SOD1-positive chondrocytes in each group (n = 5). (I-K) Quantification of NRF2-positivity, HO-1-positivity, and NQO1-positivity in chondrocytes in different groups (n = 5). Data represent mean ± S.D. **P < 0.01, ***P < 0.001 versus the Sham group. #P < 0.05, ##P < 0.01, ###P < 0.001 versus the PBS group. \$P < 0.05, \$\$P < 0.01 versus the norm-CGMs group.

potential, current studies using different tissues-sourced MSCs have shown potential capability in cartilage repair and OA treatment [50–52]. However, the tissues generated by chondrogenic differentiation of MSCs have difficulty in maintaining the phenotype of hyaline cartilage and are mostly tend to form fibrous tissue and undergo hypertrophy *in vivo*, which leads to inferior formation of functional articular cartilage. Moreover, previous studies demonstrated that MSCs tend to vascularize or ossify and are replaced by osseous tissue finally, which indicates that the chondrogenic differentiation of MSCs represents a transient stage [41]. Additionally, several clinical studies showed that intra-articular injection of MSCs is not superior to the placebo in pain relief and joint

function improvement for knee OA patients with obvious symptoms. Recently, some studies showed that CPCs derived from the superficial layer of articular cartilage are optimal cells for cartilage repair and regeneration because of strong self-proliferative capacity and great chondrogenic ability [13,40,41]. Previous study revealed that the chondrogenic differentiation degree of CPCs was higher than that of bone marrow-derived MSCs, indicating that CPCs exhibit a stronger chondrogenic capacity than MSCs [41]. In addition, a comparative study demonstrated CPCs produced lower level of the hypertrophy biomarker Collagen X in cartilage than MSCs [41]. Moreover, CPCs can form stratified tissues in cartilage repair and regeneration. Overall, these

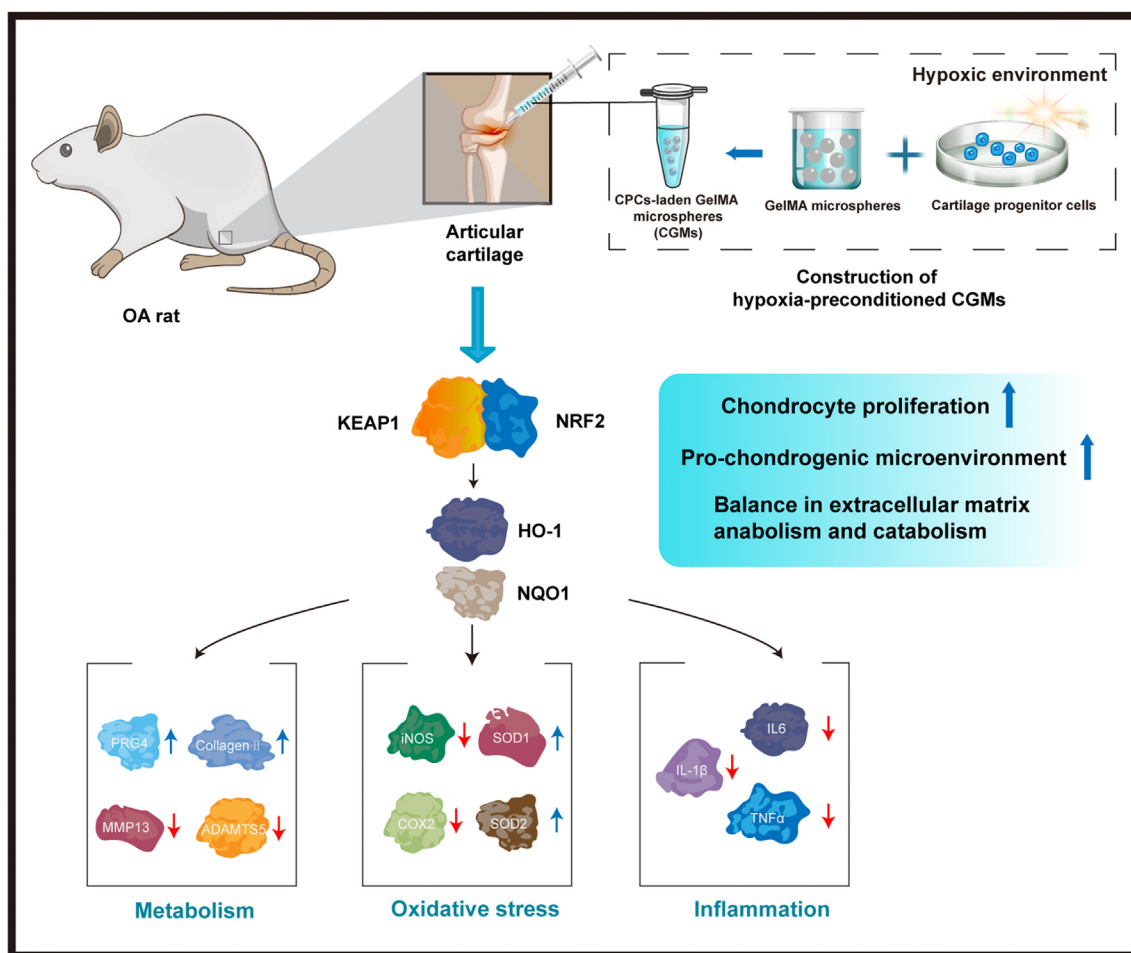


Fig. 8. Schematic illustration of the mechanism for the chondro-protective effects of hypoxia-conditioned CGMs in OA cartilage. Intra-articular injection of hypoxia-preconditioned CGMs promotes chondrocyte proliferation and extracellular matrix anabolism, inhibits inflammatory response and oxidative stress, and ultimately alleviates cartilage destruction in OA cartilage.

studies indicated CPC is a promising cell source for cartilage repair and OA treatment. Thus, CPCs were chosen as seeding cells for cartilage tissue engineering in our study. For another, the effective delivery of therapeutic CPCs is prerequisite to promote the regeneration of damaged cartilage. In this study, an injectable and biocompatible GMs delivery system was constructed to culture CPCs and our results showed that this CPCs-based therapy exhibited a strong chondrogenic ability and chondro-protective effects in both subacute and chronic OA rat models.

The conventional method for stem cells-based tissue engineering is mainly based on 2D culture technology where stem cells adhere on substrate as a monolayer. However, 2D culture cannot simulate the practical physiological conditions of stem cells niche and this severely limits the therapeutic efficacy and impedes the clinical translation of stem cells-based therapy. 3D culture system can mimic a more actual cellular physiological condition through the elaborate interactions of cell to cell and cell to extracellular matrix [17,22,23]. In addition, previous studies have indicated that 3D cultured MSCs possessed enhanced stemness and improved therapeutic effects [22,23]. Therefore, it is instructive to maintain the physiological features of CPCs and maximize the efficacy of CPCs by using 3D culture system. In this study, to more accurately mimic the natural growth condition of CPCs and keep their chondrogenic capacity as much as possible, CPCs were cultured in 3D environment by using GMs. Our results showed that GMs were suitable for CPCs culture due to their excellent biocompatibility and enhanced chondrogenic ability of CPCs.

It is known that articular cartilage is a highly differentiated tissue that lacks blood vessels, leading to a hypoxic physiological

microenvironment. Thus, we need to maintain the hypoxic culture condition of CPCs *in vitro* to maximize the chondrogenic capacity and therapeutic efficacy of CPCs. Furthermore, several studies have demonstrated that hypoxia effectively enhance the therapeutic effects of MSCs, as hypoxic condition can increase the production of regulatory factors in MSCs [24,26,27]. In this work, we found hypoxia-preconditioned CGMs showed an enhanced chondrogenic ability and chondro-protective effects *in vitro*, compared to the normoxia-pretreated CGMs group. In animal studies, we found both hypoxia-preconditioned CGMs and normoxia-pretreated CGMs can ameliorated OA progression and maintained matrix metabolism balance in both subacute and chronic OA rat models. Additionally, some *in vivo* results demonstrated that hypoxia-preconditioned CGMs exerted an improved chondro-protective effects than normoxia-pretreated CGMs, while some results showed there is no significant difference between the two groups. However, the specific mean values of the hypo-CGMs group were closer to the Sham group, compared to the norm-CGMs group. On the other hand, the individual difference is commonly existed in animal experiments and histological analysis.

The OA pathogenesis is generally associated with excessive oxidative stress and chronic inflammatory response. Both mechanical factors and aging could promote excessive oxidative stress in chondrocytes, which further cause inflammatory response, cellular senescence, and chondrocyte apoptosis in articular cartilage by regulating downstream pathways [53,54]. Previous animal studies demonstrated that inhibition of oxidative stress could attenuate OA cartilage degeneration and is a promising therapeutic strategy for OA patients [45,55]. In the present

study, we showed that hypoxia-pretreated CGMs significantly inhibited oxidative stress and promoted the production of antioxidant enzymes *in vitro* and *in vivo*. Moreover, we also found that hypoxia-pretreated CGMs effectively ameliorated inflammatory response and alleviated OA-related pain in subacute and chronic OA rats. NRF2/HO-1 is a classic and important pathway that regulates adaptive response to oxidative stress [56,57]. NRF2 participates in the regulation of downstream antioxidant markers HO-1 and NQO1. Moreover, NRF2 also regulates the levels of MDA and SOD. Additionally, KEAP1 is usually regarded as a molecular switch for NRF2 when cells suffer from excessive oxidative stress. Thus, regulation of NRF2/HO-1 pathway could inhibit excessive oxidative stress in cartilage and could be a promising therapeutic treatment for OA patients. Our *in vitro* and *in vivo* results demonstrated that hypoxia-pretreated CGMs effectively promoted the activation of NRF2/HO-1 pathway in chondrocytes.

This work provides proof of concept that 3D cultured CPCs under hypoxic condition can be used to promote OA cartilage repair and regeneration. However, there are several challenges and limitations need to be overcome in our study. Firstly, the major concern is the difficulty in obtaining large amounts of functional and standard CPCs to construct 3D cultured CGMs. As seeding cells for cartilage repair and regeneration, the current technique for obtaining a large number of CPCs is immature. A recent study found that there is a large quantity of CPCs in the perichondrium of rabbit ears, and that was thought to be a better source of CPCs [58]. That means CPCs can be obtained from various tissues such as auricular cartilage and costal cartilage. Besides, CPCs can be produced by inducing the chondrogenic differentiation of induced pluripotent stem cells (iPSCs) or embryonic stem cells (ESCs). However, the chondrogenic ability and chondro-protective effects of these different CPCs need to be further investigated. In addition, the porous microspheres possess unique advantage as these microspheres allow extensive ECM deposition or cell-cell interactions and we can further compare the chondrogenic ability between GelMA crosslinked microspheres and porous microspheres in future studies. Moreover, in animal studies, the CPCs-only control group was not performed for a comparison. Furthermore, the NRF2/HO-1 pathway is one signaling pathway in the antioxidant and chondro-protective effects in OA cartilage, whether other signaling pathways are involved in the regulation of hypoxia-pretreated CGMs need further investigation. Additionally, in animal studies, hypo-CGMs were injected into joint cavity 7 days (subacute OA model) or 14 days (chronic OA model) after OA induction in rat. Our studies demonstrated hypo-CGMs effectively ameliorated cartilage degeneration in subacute and chronic OA rat models. These results indicated that hypo-CGMs could be an effective therapy to middle- and late-stage of OA patients, but further detailed investigation about the effective dose, injection frequency, biocompatibility, and pharmacokinetics of this therapy in large animal models are necessary.

5. Conclusion

In conclusion, a 3D hypoxic CPCs culture system was successfully constructed in our study. Our findings demonstrated that 3D cultured CPCs under hypoxic condition exhibited stronger chondrogenic capacity than normoxia-pretreated 3D CPCs and 2D cultured CPCs. Additionally, hypoxia-preconditioned CGMs effectively promoted chondrocyte proliferation, rescued cartilage degeneration, and maintained cartilage matrix metabolism balance. Moreover, we showed that hypoxia-preconditioned CGMs significantly attenuated inflammation and oxidative stress by activating NRF2/HO-1 pathway *in vitro* and *in vivo* (Fig. 8). Therefore, this novel CPCs delivery system should be considered a potential therapeutic strategy for OA treatment.

Author contributions

Kai Feng: Methodology, Investigation, Writing – original draft, Writing – review & editing, Funding acquisition. **Yifan Yu:** Investigation.

Zhengsheng Chen: Investigation. **Feng Wang:** Investigation. **Kunqi Zhang:** Investigation. **Hongfang Chen:** Investigation. **Jia Xu:** Conceptualization, Writing – review & editing. **Qinglin Kang:** Conceptualization, Writing – review & editing, Supervision, Funding acquisition.

Declaration of competing interest

The authors declare that they have no known competing financial interests or personal relationships that could have appeared to influence the work reported in this paper.

Data availability

Data will be made available on request.

Acknowledgement

This study was funded by the Shanghai Sailing Program (23YF1432300), the National Natural Science Foundation of China (82072421) and the Natural Science Foundation of Shanghai (20ZR1442200).

Appendix A. Supplementary data

Supplementary data to this article can be found online at <https://doi.org/10.1016/j.mtbio.2023.100637>.

References

- [1] A. Latourte, M. Kloppenburg, P. Richette, Emerging pharmaceutical therapies for osteoarthritis, *Nat. Rev. Rheumatol.* 16 (12) (2020) 673–688.
- [2] T. Hodgkinson, D.C. Kelly, C.M. Curtin, F.J. O'Brien, Mechanosignalling in cartilage: an emerging target for the treatment of osteoarthritis, *Nat. Rev. Rheumatol.* 18 (2) (2022) 67–84.
- [3] L. Zheng, Z. Zhang, P. Sheng, A. Mobasher, The role of metabolism in chondrocyte dysfunction and the progression of osteoarthritis, *Ageing Res. Rev.* 66 (2021), 101249.
- [4] Z. Peng, H. Sun, V. Bunpetch, Y. Koh, Y. Wen, D. Wu, H. Ouyang, The regulation of cartilage extracellular matrix homeostasis in joint cartilage degeneration and regeneration, *Biomaterials* 268 (2021), 120555.
- [5] J. Gao, Z. Xia, H.B. Mary, J. Joseph, J.N. Luo, N. Joshi, Overcoming barriers for intra-articular delivery of disease-modifying osteoarthritis drugs, *Trends Pharmacol. Sci.* 43 (3) (2022) 171–187.
- [6] J.K. Lee, D.J. Responde, D.D. Cissell, J.C. Hu, J.A. Nolte, K.A. Athanasiou, Clinical translation of stem cells: insight for cartilage therapies, *Crit. Rev. Biotechnol.* 34 (1) (2014) 89–100.
- [7] Q. Ma, J. Liao, X. Cai, Different sources of stem cells and their application in cartilage tissue engineering, *Curr. Stem Cell Res. Ther.* 13 (7) (2018) 568–575.
- [8] P. Kangari, T. Talei-Khozani, I. Razeghian-Jahromi, M. Razmkhah, Mesenchymal stem cells: amazing remedies for bone and cartilage defects, *Stem Cell Res. Ther.* 11 (1) (2020) 492.
- [9] Z.M. Jessop, A. Al-Sabah, I.N. Simoes, S.E.A. Burnell, I.L. Pieper, C.A. Thornton, I.S. Whitaker, Isolation and characterisation of nasoseptal cartilage stem/progenitor cells and their role in the chondrogenic niche, *Stem Cell Res. Ther.* 11 (1) (2020) 177.
- [10] V.P. Mantripragada, W.A. Bova, N.S. Piuizzi, C. Boehm, N.A. Obuchowski, R.J. Midura, G.F. Muschler, Native-osteoarthritic joint resident stem and progenitor cells for cartilage cell-based therapies: a quantitative comparison with respect to concentration and biological performance, *Am. J. Sports Med.* 47 (14) (2019) 3521–3530.
- [11] E. Vinod, R. Parameswaran, S. Manickam Amirtham, A. Livingston, B. Ramasamy, U. Kachroo, Comparison of the efficiency of laminin versus fibronectin as a differential adhesion assay for isolation of human articular cartilage derived chondroprogenitors, *Connect. Tissue Res.* 62 (4) (2021) 427–435.
- [12] E. Vinod, R. Parameswaran, B. Ramasamy, U. Kachroo, Pondering the potential of hyaline cartilage-derived chondroprogenitors for tissue regeneration: a systematic review, *Cartilage* 13 (2_suppl) (2021) 34S–52S.
- [13] J. Kim, A.N. Tran, J.Y. Lee, S.H. Park, S.R. Park, B.H. Min, B.H. Choi, Human Fetal Cartilage-Derived Progenitor Cells Exhibit Anti-inflammatory Effect on IL-1beta-Mediated Osteoarthritis Phenotypes *In Vitro*, *Tissue Eng Regen Med*, 2022.
- [14] R. Levato, W.R. Webb, I.A. Otto, A. Mensinga, Y. Zhang, M. van Rijen, R. van Weeren, I.M. Khan, J. Malda, The bio in the ink: cartilage regeneration with bioprintable hydrogels and articular cartilage-derived progenitor cells, *Acta Biomater.* 61 (2017) 41–53.
- [15] K. Xue, X. Zhang, Z. Gao, W. Xia, L. Qi, K. Liu, Cartilage progenitor cells combined with PHBV in cartilage tissue engineering, *J. Transl. Med.* 17 (1) (2019) 104.

- [16] Y. Zhang, M. Chopp, Z.G. Zhang, M. Katakowski, H. Xin, C. Qu, M. Ali, A. Mahmood, Y. Xiong, Systemic administration of cell-free exosomes generated by human bone marrow derived mesenchymal stem cells cultured under 2D and 3D conditions improves functional recovery in rats after traumatic brain injury, *Neurochem. Int.* 111 (2017) 69–81.
- [17] M. Han, H. Yang, X. Lu, Y. Li, Z. Liu, F. Li, Z. Shang, X. Wang, X. Li, J. Li, H. Liu, T. Xin, Three-dimensional-cultured MSC-derived exosome-hydrogel hybrid microneedle array patch for spinal cord repair, *Nano Lett.* 22 (15) (2022) 6391–6401.
- [18] S.Y. Lee, J.W. Lee, 3D spheroid cultures of stem cells and exosome applications for cartilage repair, *Life* 12 (7) (2022).
- [19] E. Gara, E. Zucchelli, A. Nemes, Z. Jakus, K. Ajtay, E. Kemececi, G. Kiszler, N. Hegedus, K. Szigeti, I. Foldes, K. Arvai, J. Kosa, K. Kolev, E. Komorowicz, P. Padmanabhan, P. Maurovich-Horvat, E. Dosa, G. Varady, M. Polos, I. Hartyanszky, S.E. Harding, B. Merkely, D. Mathe, G. Szabo, T. Radovits, G. Foldes, 3D culturing of human pluripotent stem cells-derived endothelial cells for vascular regeneration, *Theranostics* 12 (10) (2022) 4684–4702.
- [20] Y. Yuan, X. Zhang, Y. Zhan, S. Tang, P. Deng, Z. Wang, J. Li, Adipose-derived stromal/stem cells are verified to be potential seed candidates for bio-root regeneration in three-dimensional culture, *Stem Cell Res. Ther.* 13 (1) (2022) 234.
- [21] P. Cui, P. Pan, L. Qin, X. Wang, X. Chen, Y. Deng, X. Zhang, Nanoengineered hydrogels as 3D biomimetic extracellular matrix with injectable and sustained delivery capability for cartilage regeneration, *Bioact. Mater.* 19 (2023) 487–498.
- [22] Y. Xie, L. Sutrisno, T. Yoshitomi, N. Kawazoe, Y. Yang, G. Chen, Three-dimensional culture and chondrogenic differentiation of mesenchymal stem cells in interconnected collagen scaffolds, *Biomed. Mater.* 17 (3) (2022).
- [23] S.H. Bogers, J.G. Barrett, Three-dimensional culture of equine bone marrow-derived mesenchymal stem cells enhances anti-inflammatory properties in a donor-dependent manner, *Stem Cell. Dev.* 31 (23–24) (2022 Dec) 777–786.
- [24] Y. Yang, E.H. Lee, Z. Yang, Hypoxia-conditioned mesenchymal stem cells in tissue regeneration application, *Tissue Eng. B Rev.* 28 (5) (2022) 966–977.
- [25] M. Carmona, L.M. Paco-Meza, R. Ortega, S. Canadillas, J. Caballero-Villarraso, A. Blanco, C. Herrera, Hypoxia preconditioning increases the ability of healthy but not diabetic rat-derived adipose stromal/stem cells (ASC) to improve histological lesions of streptozotocin-induced diabetic nephropathy, *Pathol. Res. Pract.* 230 (2022), 153756.
- [26] K. Archacka, I. Grabowska, B. Mierzejewski, J. Graffstein, A. Gorzynska, M. Krawczyk, A.M. Rozycka, I. Kalaszczynska, G. Muras, W. Streminska, K. Janczyk-Illach, P. Walczak, M. Janowski, M.A. Ciemerych, E. Brzoska, Hypoxia preconditioned bone marrow-derived mesenchymal stromal/stem cells enhance myoblast fusion and skeletal muscle regeneration, *Stem Cell Res. Ther.* 12 (1) (2021) 448.
- [27] X. Peng, B. Liang, H. Wang, J. Hou, Q. Yuan, Hypoxia pretreatment improves the therapeutic potential of bone marrow mesenchymal stem cells in hindlimb ischemia via upregulation of NRG-1, *Cell Tissue Res.* 388 (1) (2022) 105–116.
- [28] C.K.I. Ranmuthu, C.D.S. Ranmuthu, C.K. Wijewardena, M.K.T. Seah, W.S. Khan, Evaluating the effect of hypoxia on human adult mesenchymal stromal cell chondrogenesis in vitro: a systematic review, *Int. J. Mol. Sci.* 23 (2022).
- [29] A. Nowak-Stepniowska, P.N. Osuchowska, H. Fiedorowicz, E.A. Trafny, Insight in hypoxia-mimetic agents as potential tools for mesenchymal stem cell priming in regenerative medicine, *Stem Cell. Int.* 2022 (2022), 8775591.
- [30] Y. Lu, L. Wei, X. Zhang, J. Cai, Y. Zhu, J. Xiao, Y. Duan, H. Liu, Z. Wang, S. Li, The regulation of mesenchymal stem cell therapy through magnetic resonance imaging agents-based cellular condition and oxygen environment, *J. Biomed. Nanotechnol.* 14 (11) (2018) 1906–1920.
- [31] D. Cai, W. Feng, J. Liu, L. Jiang, S. Chen, T. Yuan, C. Yu, H. Xie, D. Geng, J. Qin, 7,8-Dihydroxyflavone activates Nrf2/HO-1 signaling pathways and protects against osteoarthritis, *Exp. Ther. Med.* 18 (3) (2019) 1677–1684.
- [32] X. Zhou, Y. Zhang, M. Hou, H. Liu, H. Yang, X. Chen, T. Liu, F. He, X. Zhu, Melatonin prevents cartilage degradation in early-stage osteoarthritis through activation of miR-146a/NRF2/HO-1 Axis, *J. Bone Miner. Res.* 37 (5) (2022) 1056–1072.
- [33] L. Luo, F. Huang, S. Zhong, R. Ding, J. Su, X. Li, Astaxanthin attenuates ferroptosis via Keap1-Nrf2/HO-1 signaling pathways in LPS-induced acute lung injury, *Life Sci.* 311 (Pt A) (2022), 121091.
- [34] W. Qiu, X. Zhang, X. Pang, J. Huang, S. Zhou, R. Wang, Z. Tang, R. Su, Asiatic acid alleviates LPS-induced acute kidney injury in broilers by inhibiting oxidative stress and ferroptosis via activation of the Nrf2 pathway, *Food Chem. Toxicol.* 170 (2022), 113468.
- [35] X.X. Yang, R. Yang, F. Zhang, Role of Nrf2 in Parkinson's disease: toward new perspectives, *Front. Pharmacol.* 13 (2022), 919233.
- [36] Q. Xiang, Y. Zhao, J. Lin, S. Jiang, W. Li, The Nrf2 antioxidant defense system in intervertebral disc degeneration: molecular insights, *Exp. Mol. Med.* 54 (8) (2022) 1067–1075.
- [37] X.H. Xue, J.X. Xue, W. Hu, F.L. Shi, Y. Yang, Nomilin targets the Keap1-Nrf2 signalling and ameliorates the development of osteoarthritis, *J. Cell Mol. Med.* 24 (15) (2020) 8579–8588.
- [38] W. Zhu, H. Tang, J. Li, R.M. Guedes, L. Cao, C. Guo, Ellagic acid attenuates interleukin-1beta-induced oxidative stress and exerts protective effects on chondrocytes through the Kelch-like ECH-associated protein 1 (Keap1)/Nuclear factor erythroid 2-related factor 2 (Nrf2) pathway, *Bioengineered* 13 (4) (2022) 9233–9247.
- [39] J. Jin, X. Lv, B. Wang, C. Ren, J. Jiang, H. Chen, X. Chen, M. Gu, Z. Pan, N. Tian, A. Wu, L. Sun, W. Gao, X. Wang, X. Zhang, Y. Wu, Y. Zhou, Limonin inhibits IL-1beta-induced inflammation and catabolism in chondrocytes and ameliorates osteoarthritis by activating Nrf2, *Oxid. Med. Cell. Longev.* 2021 (2021), 7292512.
- [40] K. Wang, J. Li, Z. Li, B. Wang, Y. Qin, N. Zhang, H. Zhang, X. Su, Y. Wang, H. Zhu, Chondrogenic progenitor cells exhibit superiority over mesenchymal stem cells and chondrocytes in platelet-rich plasma scaffold-based cartilage regeneration, *Am. J. Sports Med.* 47 (9) (2019) 2200–2215.
- [41] J. Gu, B. Wang, T. Wang, N. Zhang, H. Liu, J. Gui, Y. Lu, Effects of cartilage progenitor cells, bone marrow mesenchymal stem cells and chondrocytes on cartilage repair as seed cells: an in vitro study, *Drug Des. Dev. Ther.* 16 (2022) 1217–1230.
- [42] J. Wu, L. Kuang, C. Chen, J. Yang, W.N. Zeng, T. Li, H. Chen, S. Huang, Z. Fu, J. Li, R. Liu, Z. Ni, L. Chen, L. Yang, miR-100-5p-abundant exosomes derived from infrapatellar fat pad MSCs protect articular cartilage and ameliorate gait abnormalities via inhibition of mTOR in osteoarthritis, *Biomaterials* 206 (2019) 87–100.
- [43] K. Feng, X. Xie, J. Yuan, L. Gong, Z. Zhu, J. Zhang, H. Li, Y. Yang, Y. Wang, Reversing the surface charge of MSC-derived small extracellular vesicles by epsilonPL-PG-DSPE for enhanced osteoarthritis treatment, *J. Extracell. Vesicles* 10 (13) (2021), e12160.
- [44] K. Feng, Y. Ge, Z. Chen, X. Li, Z. Liu, X. Li, H. Li, T. Tang, F. Yang, X. Wang, Curcumin inhibits the PERK-eIF2alpha-CHOP pathway through promoting SIRT1 expression in oxidative stress-induced rat chondrocytes and ameliorates osteoarthritis progression in a rat model, *Oxid. Med. Cell. Longev.* 2019 (2019), 8574386.
- [45] K. Feng, Z. Chen, L. Pengcheng, S. Zhang, X. Wang, Quercetin attenuates oxidative stress-induced apoptosis via SIRT1/AMPK-mediated inhibition of ER stress in rat chondrocytes and prevents the progression of osteoarthritis in a rat model, *J. Cell. Physiol.* 234 (10) (2019) 18192–18205.
- [46] W. Zhu, H. Tang, L. Cao, J. Zhang, J. Li, D. Ma, C. Guo, Epigallocatechin-3-O-gallate ameliorates stress-induced chondrocyte dysfunction and exerts chondroprotective effects via the Keap1/Nrf2/ARE signaling pathway, *Chem. Biol. Drug Des.* 100 (1) (2022) 108–120.
- [47] C.H. Woo, H.K. Kim, G.Y. Jung, Y.J. Jung, K.S. Lee, Y.E. Yun, J. Han, J. Lee, W.S. Kim, J.S. Choi, S. Yang, J.H. Park, D.G. Jo, Y.W. Cho, Small extracellular vesicles from human adipose-derived stem cells attenuate cartilage degeneration, *J. Extracell. Vesicles* 9 (1) (2020), 1735249.
- [48] N. Gerwin, A.M. Bendele, S. Glasson, C.S. Carlson, The OARSI histopathology initiative - recommendations for histological assessments of osteoarthritis in the rat, *Osteoarthritis Cartilage* 18 (Suppl 3) (2010) S24–S34.
- [49] D. Kang, J. Lee, J. Jung, B.A. Carlson, M.J. Chang, C.B. Chang, S.B. Kang, B.C. Lee, V.N. Gladyshev, D.L. Hatfield, B.J. Lee, J.H. Kim, Selenophosphate synthetase 1 deficiency exacerbates osteoarthritis by dysregulating redox homeostasis, *Nat. Commun.* 13 (1) (2022) 779.
- [50] W.Y. Lee, B. Wang, Cartilage repair by mesenchymal stem cells: clinical trial update and perspectives, *J Orthop Translat* 9 (2017) 76–88.
- [51] S.M. Richardson, G. Kalamegam, P.N. Pushparaj, C. Matta, A. Memic, A. Khademhosseini, R. Mobasher, F.L. Poletti, J.A. Hoyland, A. Mobasher, Mesenchymal stem cells in regenerative medicine: focus on articular cartilage and intervertebral disc regeneration, *Methods* 99 (2016) 69–80.
- [52] C. De Bari, A.J. Roelofs, Stem cell-based therapeutic strategies for cartilage defects and osteoarthritis, *Curr. Opin. Pharmacol.* 40 (2018) 74–80.
- [53] M.Y. Ansari, N. Ahmad, T.M. Haqqi, Oxidative stress and inflammation in osteoarthritis pathogenesis: role of polyphenols, *Biomed. Pharmacother.* 129 (2020), 110452.
- [54] P. Lepetos, A.G. Papavassiliou, ROS/oxidative stress signaling in osteoarthritis, *Biochim. Biophys. Acta* 1862 (4) (2016) 576–591.
- [55] B. Poulet, F. Beier, Targeting oxidative stress to reduce osteoarthritis, *Arthritis Res. Ther.* 18 (2016) 32.
- [56] I. Bellezza, I. Giambanco, A. Minelli, R. Donato, Nrf2-Keap1 signaling in oxidative and reductive stress, *Biochim. Biophys. Acta Mol. Cell Res.* 1865 (5) (2018) 721–733.
- [57] Q. Ma, Role of nrf2 in oxidative stress and toxicity, *Annu. Rev. Pharmacol. Toxicol.* 53 (2013) 401–426.
- [58] T. Togo, A. Utani, M. Naitoh, M. Ohta, Y. Tsuji, N. Morikawa, M. Nakamura, S. Suzuki, Identification of cartilage progenitor cells in the adult ear perichondrium: utilization for cartilage reconstruction, *Lab. Invest.* 86 (5) (2006) 445–457.